LETTER Communicated by Terrence Sejnowski

Strong Allee Effect Synaptic Plasticity Rule in an Unsupervised Learning Environment

Eddy Kwessi
ekwessi@trinity.edu
Department of Mathematics, Trinity University, San Antonio, TX 78212, U.S.A.

Synaptic plasticity, or the ability of a brain to change one or more of its functions or structures at the synaptic level, has generated and is still generating a lot of interest from the scientific community especially from neuroscientists. These interests went into high gear after empirical evidence was collected that challenged the established paradigm that human brain structures and functions are set from childhood and only modest changes were expected beyond. Early synaptic plasticity rules or laws to that regard include the basic Hebbian rule that proposed a mechanism for strengthening or weakening of synapses (weights) during learning and memory. This rule, however, did not account for the fact that weights must have bounded growth over time. Thereafter, many other rules that possess other desirable properties were proposed to complement the basic Hebbian rule. In particular, a desirable property in a synaptic plasticity rule is that the ambient system must account for inhibition, which is often achieved if the rule used allows for a lower bound in synaptic weights. To that regard, in this letter, we propose such a synaptic plasticity rule that is inspired by the Allee effect, a phenomenon often observed in population dynamics. We show that properties such as synaptic normalization, competition between weights, decorrelation potential, and dynamic stability are satisfied. We show that in fact, an Allee effect in synaptic plasticity can be construed as an absence of plasticity.

1 Introduction

Synapses play an important role in the brain because they are junctions between the nerves cells. As such, they facilitate the diffusion of chemical substances called neurotransmitters from the brain to other parts of the body. During this diffusion, synapses are sometimes modified to adapt to the impulses and their transmission rate. These synaptic modifications may be due to lived experience and training and can occur at functional and structural levels. At the functional level, the brain may move functions from one area to other areas, often from damaged to undamaged ones. At the structural level, the brain may actually change its physical structure, mainly some synaptic structures as a result of external activities. Modifications of

Neural Computation **35, 1–34** (2023)
https://doi.org/10.1162/neco_a_01577

synapses can in turn affect behavior and training; therefore, understanding the dichotomy between synaptic modifications and experience and/or training is paramount if one wants to have an insight into some brain activities. Brain plasticity or neuroplasticity can be thought of as the ability of the brain to adapt to external activities by reorganizing some of its pathways or modifying some of its synaptic structure.

Early researchers on synaptic plasticity include Hebb (1949), who conjectured that on one hand, synapses from two neurons are often strengthened if impulses from one neuron contribute to the firing of another. On the other hand, synapses are weakened if noncoincidental neuronal firings occur. In essence, this rule infers that synaptic modifications are in direct relationship with experience and training, and consequently, the mechanisms underlying learning and memory can be understood via these synaptic modifications. In fact, there is ample empirical evidence consisting of transient and long-lasting effects (long-term potentiation and depression) starting with Bliss and Lomo (1973), who experimented plasticity in rabbits. Plasticity was later experimented in selected regions of the brains, including the hippocampus neocortex and cerebellum (Bear & Malenka, 1994; Bliss & Lomo, 1973; Bussey, 2011; Feldman, 2009; Liu & Nusslock, 2018a, 2018b; Olson et al., 2006; Siegelbaum & Kandel, 1991; Xu & Kang, 2005).

However, to understand plasticity at the functional level, one needs to go beyond mechanistic models as described above and find how plasticity relates neurons and/or networks of neurons to the basic rules that govern its induction (Dayan & Abbott, 2001). This entails finding mechanisms relating the strengthening or weakening of synapses via neurotransmitters and (presynaptic) neurons. Many mathematical models or synaptic plasticity rules have been proposed to explain synaptic plasticity in supervised and unsupervised learning environments. In an unsupervised learning environment where the neuron network self-organizes, an activity is represented by a continuous variable (input) at the presynaptic level and linked to a postsynaptic activity variable (output) by dynamic weights. The relationship between these variables is a differential equation describing the change of weights over time and include and is not limited to the basic Hebbian rule (Sejnowski & Tesauro, 1989) and its variant, the covariance rule (Dayan & Abbott, 2001), the Bienestock-Cooper-Munro (BCM) rule (Bienenstock et al., 1982), and the Oja rule (Oja, 1982). To avoid unbounded growth, an upper saturation limit is often imposed, for instance in BCM and Oja rules. A lower limit is needed to allow for inhibition. However, this lower limit is often given by the condition that the length of weights not be zero. In population dynamics, there are rules for which the density or size of a population is both bounded above and below by nonnegative constants as in the Allee effect. The Allee effect was introduced by Allee (1949) and characterizes a phenomenon in population dynamics where there is a positive correlation between a population density and its per capita growth rate. Allee effects are divided into strong and weak Allee effects (Hutchings, 2015). The strong

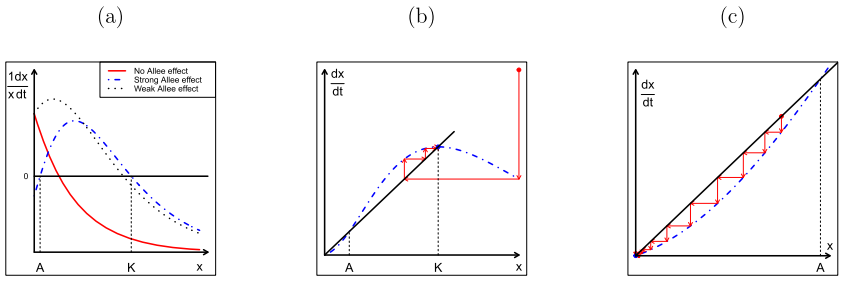

Figure 1: (a) The per capita growth rate as a function of the population density x. The red curve represents no Allee effect since there is a negative correlation between the per capita growth rate and the density. The black dashed curve represents the weak Allee effect since at lower densities x, the per capita growth rate is increasing but there is no Allee threshold A. The blue dashed represents the strong Allee effect since there is a positive correlation between the per capita growth rate and the existence of a threshold under with the population decreases to extinction. This is highlighted in the cobweb diagram in panel c where a trajectory (red arrow) starting below A converges to 0. In panel b, the starting trajectory (red arrow) above A converge to K.

Allee effect occurs when a population has a critical density A below which it declines to extinction and above which it increases toward its carrying capacity K. The weak Allee effect occurs when a population lacks such a critical density, but at lower densities, the population growth rate arises with increasing densities (see Figure 1). Since their inception, Allee effects have substantially been investigated and applied by researchers across the board.

Mathematical models of the Allee effects and their dynamics have been investigated for competing populations in Assas et al. (2015a, 2015b, 2014; Assas, Elaydi et al., 2015); Elaydi et al. (2018). Stochastic models of the Allee effects were discussed in Assas et al. (2016). Models addressing Allee effects and conservation are discussed in Courchamp et al. (2008). Models addressing population resilience were proposed by Dennis et al. (2015). Some real-life evidence of Allee effects has been documented in Courchamp et al. (2008) and Perala and Kuparinen (2017). Possible extensions of Allee effects to medicine have been proposed in Delitala and Ferraro (2020), Fontanari and Perlovsky (2006), Johnson et al. (2019), Konstorum et al. (2016), and Neufeld et al. (2017).

To our knowledge, the Allee effect has not yet been been discussed in combination with plasticity rules. In this letter, we aim to make a foray into the topic and show that in fact, an Allee effect, when combined with the Oja rule, can be characterized as a drift toward an absence of plasticity. Moreover, the model we propose has the following key advantages.

1. Unbounded growth is controlled and normalization is preserved.
2. Blow-up is avoided at lower initial values.
3. Competition between weights is induced.
4. The model is general enough to account for multiple layers of pre- and postsynaptic neurons.
5. Under specific conditions on the network parameters, stability of the dynamical system is obtained.

The use of an Allee effect in neuroscience may have the potential to produce invaluable information that highlight hidden features in plasticity and could potentially enrich the ever growing literature on the topic. The remainder of this letter is organized as follows. In section 3, we introduce our idea of an Allee effect postsynaptic neuron model. In section 4, we provide a stability analysis of a single postsynaptic neuron model with and without a plastic recurrent connection. Ensembles of postsynaptic neurons are tackled in section 5.

2 Preliminaries

Consider a system with L layers and let an $L \times N_u$ matrix $\mathbf{u} = \left(\mathbf{u}^{(1)}, \mathbf{u}^{(2)}, \ldots, \mathbf{u}^{(L)}\right)$ represent the presynaptic activities in the system. For $1 \le \ell \le L$, $\mathbf{u}^{(\ell)} = \left(u_1^{(\ell)}, u_2^{(\ell)}), \ldots, u_{N_u}^{(\ell)}\right)$ represents presynaptic activities of N_u inputs or neurons within the ℓth layer of the system. Let an $L \times N_v$ matrix $\mathbf{v} = \left(\mathbf{v^{(1)}}, \mathbf{v^{(2)}}, \ldots, \mathbf{v^{(L)}}\right)$ be the postsynaptic activities generated by the presynaptic activities $\mathbf{u}$, where $\mathbf{v}^{(\ell)} = \left(v_1^{(\ell)}, v_2^{(\ell)}, \ldots, v_{N_v}^{(\ell)}\right)$ represents the postsynaptic activities of N_v neurons on the ℓth layer. Let $\mathbf{W}$ be an input synaptic block matrix of weights representing the strengths of the synapses from the presynaptic neurons $\mathbf{u}$ to the postsynaptic neurons $\mathbf{v}$. We note that $\mathbf{W}$ is an $L \times N_u \times L \times N_v$ block matrix with entries $\left(\mathbf{W}^{(k,\ell)}\right)$, for $1 \le k, \ell \le L$. Each block $\mathbf{W}^{(k,\ell)}$ is a matrix with entries $w_{ij}^{(k,\ell)}$ where $1 \le j \le N_v$ and $1 \le i \le N_u$. To account for interconnections between postsynaptic neurons, we consider an $L \times N_v \times L \times N_v$ recurrence block-matrix $\mathbf{Z}$ with entries $\mathbf{Z}^{(k,\ell)}$, for $1 \le k, \ell \le L$, where each entry $\mathbf{Z}^{(k,\ell)}$ is a matrix with entries $z_{mj}^{(k,\ell)}$ for $1 \le j, m \le N_v$. We let $d_w = L \times N_u \times L \times N_v$ and $d_z = L \times N_v \times L \times N_v$ and we define the length of a vector $\mathbf{W}$ in $\mathbb{R}^{d_w}$ as $\|\mathbf{W}\|^2 = \mathbf{W^T} \cdot \mathbf{W}$, where the dot stands for the dot or inner product in $\mathbb{R}^{d_w}$ (see Figure 2).

Remark 1. In the sequel, we will invariably use the dot product with the following understanding:

$\mathbf{W}^T \cdot \mathbf{u}$ is an $L \times N_v$ matrix with entries:

$$(\mathbf{W}^T \cdot \mathbf{u})_i^{(k)} = \sum_{\ell=1}^{L} \sum_{j=1}^{N_u} w_{ij}^{(k,\ell)} u_j^{(\ell)}, \quad \text{for } 1 \le k \le L, 1 \le i \le N_v.$$

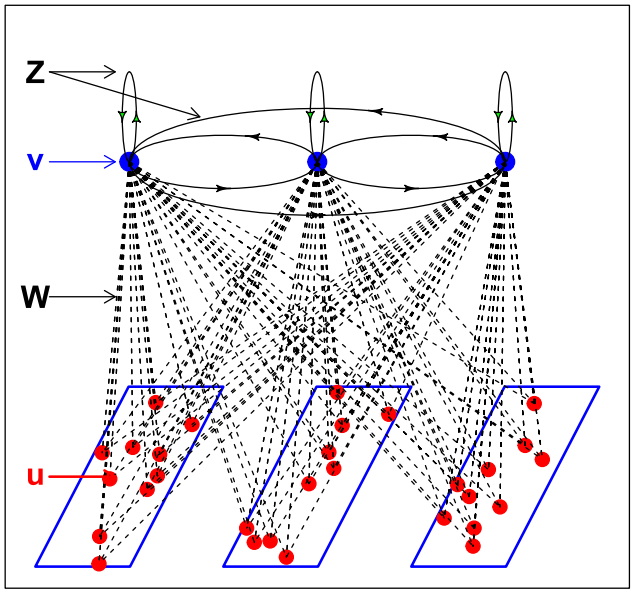

Figure 2: A geometric representation of a triple-layer architecture with $N_u = 10$ presynaptic neurons $u_j^{(\ell)}$ and $N_v = 1$ postsynaptic neurons $v_i^{(\ell)}$ per layer, $d_w = 90$ weights $w_{ik}^{(k,\ell)}$, and $d_z = 9$ recurrent connections $z_{im}^{(k,\ell)}$.

$\mathbf{Z}^T \cdot \mathbf{v}$ is an $L \times N_v$ matrix with entries:

$$(\mathbf{Z}^T \cdot \mathbf{v})_i^{(k)} = \sum_{\ell=1}^{L} \sum_{m=1}^{N_v} z_{im}^{(k,\ell)} v_m^{(\ell)} \quad \text{for } 1 \le k \le L, 1 \le i \le N_v.$$

Consequently, as sums of products of coordinates of vectors, entries for $\mathbf{W}^T \cdot \mathbf{u}$ and $\mathbf{Z}^T \cdot \mathbf{v}$ are themselves dot products and therefore enjoy their properties. Also in the sequel, matrices and vectors will be represented by boldface symbols, whereas scalars will be represented with normal font symbols. We start with some definitions.

Definition 1. *The learning activity of a system or plasticity function of a system is a function given as*

$$L(\mathbf{W}, \mathbf{u}, \mathbf{v}) = H(\mathbf{W}, \mathbf{u}, \mathbf{v}) - \varphi(\mathbf{W}, \mathbf{u}, \mathbf{v}), \tag{2.1}$$

where $H(\mathbf{W}, \mathbf{u}, \mathbf{v})$ is a function referred to as the Hebbian function and $\varphi(\mathbf{W}, \mathbf{u}, \mathbf{v})$ is a function referred to as the Hebbian modification function.

Table 1: Known Plasticity Rules

Plasticity rule	$H(\mathbf{W}, \mathbf{u}, \mathbf{v})$	$\varphi(\mathbf{W}, \mathbf{u}, \mathbf{v})$	$\tau_{\mathbf{W}} \frac{d\mathbf{W}}{dt}$	Reference
Hebbian	$\mathbf{v}^T\mathbf{u}$	0	$\mathbf{v}^T\mathbf{u}$	Hebb (1949)
Covariance	$\mathbf{v}^T\mathbf{u}$	$\theta_{\mathbf{u}}\mathbf{v}^T$	$\mathbf{v}^T(\mathbf{u}-\theta_{\mathbf{u}})$	Dayan and Abbott (2001)
		$\theta_{\mathbf{v}}\mathbf{u}$	$(\mathbf{v}^T-\theta_{\mathbf{v}})\mathbf{u}$	
BCM	$\mathbf{v}^T\mathbf{u}\mathbf{v}$	$\theta_{\mathbf{v}}\mathbf{v}^T\mathbf{u}$	$\mathbf{v}^T\mathbf{u}(\mathbf{v}-\theta_{\mathbf{v}})$	Bienenstock et al. (1982)
Oja	$\mathbf{v}^T\mathbf{u}$	$\alpha\mathbf{v}^T\mathbf{W}\mathbf{v}$	$\mathbf{v}^T\mathbf{u}-\alpha\mathbf{v}^T\mathbf{W}\mathbf{v}$	Oja (1982)

Definition 2. *We define a synaptic plasticity rule as*

$$\tau_{\mathbf{W}} \frac{d\mathbf{W}}{dt} = L(\mathbf{W}, \mathbf{u}, \mathbf{v}). \tag{2.2}$$

The constant $\tau_{\mathbf{W}}$ represents a timescaling constant controlling the rate of change of $\mathbf{W}$, and $\lambda_{\mathbf{W}} = \frac{1}{\tau_{\mathbf{W}}}$ represents the learning rate. The model in equation 2.2 is general enough to include many known synaptic plasticity rules (see Table 1).

To model the dynamics of postsynaptic neurons $\mathbf{v}$, we will use the firing-rate equation given as

$$\tau_{\mathbf{v}} \frac{d\mathbf{v}}{dt} = -\mathbf{v} + T(\mathbf{W}, \mathbf{Z}, \mathbf{u}, \mathbf{v}), \tag{2.3}$$

where $\tau_{\mathbf{v}}$ represents the timescale of the firing-rate dynamics of $\mathbf{v}$ and $T(\mathbf{W}, \mathbf{Z}, \mathbf{u}, \mathbf{v})$ is a function representing the total activity in the system. This activity may consist of pre-and postsynaptic activities $\mathbf{u}$ and $\mathbf{v}$, with feed-forward and/or feedbackward connections with intensities (or weights) $\mathbf{W}$, with or without recurrent connections with intensities $\mathbf{Z}$. In the general literature, $T(\mathbf{W}, \mathbf{Z}, \mathbf{u}, \mathbf{v})$ is often taken as a linear function of the pre- and postsynaptic activities $\mathbf{u}$ and $\mathbf{v}$. That is, $T(\mathbf{W}, \mathbf{Z}, \mathbf{u}, \mathbf{v}) = \mathbf{W^T} \cdot \mathbf{u} + \mathbf{Z^T} \cdot \mathbf{v}$. It could also be a nonlinear function depending on an activation function G as $T(\mathbf{W}, \mathbf{Z}, \mathbf{u}, \mathbf{v}) = G(\mathbf{W}^T \cdot \mathbf{u} + \mathbf{Z}^T \cdot \mathbf{v})$ or two activation functions G_1 and G_2 as $T(\mathbf{W}, \mathbf{Z}, \mathbf{u}, \mathbf{v}) = \mathbf{W}^T \cdot G_1(\mathbf{u}) + \mathbf{Z}^T \cdot G_2(\mathbf{v})$. The activation function controls the rate of signals emitted by presynaptic neurons $\mathbf{u}$ and the recurrence rate of postsynaptic neurons $\mathbf{v}$. It is common to use either the sigmoid function $G(x) = (1 + e^{-x})^{-1}$ or the Heaviside function $G(x) = 0, x < 0, G(x) = 1, x > 1$. We observe, however, that more general activation functions G can be considered (Kwessi, 2021a). We note that a more complete and perhaps more realistic model for equation 2.3 should contain a diffusion term and a less trivial reaction term than $\mathbf{v}$. For simplicity and to maintain tractability, we will will not do so in this letter.

Remark 2. It is important to note that here, the total activity, $T(\mathbf{W}, \mathbf{Z}, \mathbf{u}, \mathbf{v})$ would be zero if the the pre- and and postsynaptic activities $\mathbf{u}$ and $\mathbf{v}$ are canceling each other. This is obviously the case if $\mathbf{u} = 0$ and $\mathbf{v} = 0$. From equation 2.3, above, if $T(\mathbf{W}, \mathbf{Z}, \mathbf{u}, \mathbf{v}) = 0$, then $\mathbf{v}(t) = \mathbf{v}_0 e^{-\lambda_{\mathbf{v}} t}$ and thus approaches 0 over time. Combining the latter with equation 2.2, it follows that, for some constant presynaptic inputs $\mathbf{u}$ and for some generic constant matrix Σ that

- $\mathbf{W}(t) = \frac{\lambda_{\mathbf{W}}}{\lambda_{\mathbf{v}}}\left[e^{-\lambda_{\mathbf{v}} t}\mathbf{v}_0^T\mathbf{u} + \Sigma\right]$ for the basic Hebb rule.
- $\mathbf{W}(t) = \frac{\lambda_{\mathbf{W}}}{\lambda_{\mathbf{v}}}\left[e^{-\lambda_{\mathbf{v}} t}\mathbf{v}_0^T(\mathbf{u} - \theta_{\mathbf{v}}) + \Sigma\right]$ or $\mathbf{W}(t) = \frac{\lambda_{\mathbf{W}}}{\lambda_{\mathbf{v}}}\left[e^{-\lambda_{\mathbf{v}} t}\mathbf{v}_0^T(\theta_{\mathbf{u}} - \mathbf{u}) + \Sigma\right]$ for the covariance rule.
- $\mathbf{W}(t) = \frac{\lambda_{\mathbf{W}}}{\lambda_{\mathbf{v}}}\left[\left(\frac{e^{-\lambda_{\mathbf{v}} t}}{2}\mathbf{v}_0^T - \theta_{\mathbf{v}}\right)e^{-\lambda_{\mathbf{v}} t}\mathbf{v}_0^T\mathbf{u} + \Sigma\right]$ for the BCM rule.
- $\mathbf{W}(t) = e^{\mathbf{v}_0^T\mathbf{v}_0\frac{\alpha}{2\lambda_{\mathbf{v}}}e^{-2\lambda_{\mathbf{v}} t}}\left[\mathbf{v}_0^T\mathbf{u}\int e^{-\lambda_{\mathbf{v}} t - \mathbf{v}_0^T\mathbf{v}_0\frac{\alpha}{2\lambda_{\mathbf{v}}}e^{-2\lambda_{\mathbf{v}} t}}dt + \Sigma\right]$ for the Oja rule.

We can therefore infer that when $T(\mathbf{W}, \mathbf{Z}, \mathbf{u}, \mathbf{v}) = 0$, $\mathbf{v}$ approaches 0 over time whereas $\mathbf{W}$ approaches a constant Σ. We will restrict ourselves to the case where $T(\mathbf{W}, \mathbf{Z}, \mathbf{u}, \mathbf{v}) = \mathbf{W}^T \cdot \mathbf{u} + \mathbf{Z}^T \cdot \mathbf{v} = 0$ and $\mathbf{v} = \mathbf{0}$ if the presynaptic activities vector $\mathbf{u}$ is zero.

Remark 3. We also observe that $T(\mathbf{W}, \mathbf{Z}, \mathbf{u}, \mathbf{v}) = \mathbf{W}^T \cdot \mathbf{u} + \mathbf{Z}^T \cdot \mathbf{v}$ can be understood as the total potential energy in the system. Indeed, suppose $\mathbf{W}$, $\mathbf{Z}$, $\mathbf{u}$, and $\mathbf{v}$ are vector fields over an open connected domain $\mathscr{D}$. Let P be a path in $\mathscr{D}$. If these fields are continuous over $\mathscr{D}$ and $\int_P \mathbf{W}^T \cdot d\mathbf{u}$ and $\int_P \mathbf{u} \cdot d\mathbf{W}^T$ are path independent, then the fields $\mathbf{W}$ and $\mathbf{u}$ are conservative. Consequently, there exist functions f_1 and f_2 such that $\mathbf{W}^T = \nabla f_1$ and $\mathbf{u} = \nabla f_2$. Therefore, the potential energy due to the fields $\mathbf{W}^T$ and $\mathbf{u}$ is

$$\int_P \nabla f_1 \cdot d\mathbf{u} + \int_P \nabla f_2 \cdot d\mathbf{W} = \mathbf{W}^T \cdot \mathbf{u}.$$

Similarly, there exist functions g_1 and g_2 such that the potential energy due to the fields $\mathbf{Z}$ and $\mathbf{v}$ is

$$\int_P \nabla g_1 \cdot d\mathbf{v} + \int_P \nabla g_2 \cdot d\mathbf{Z}^T = \mathbf{Z}^T \cdot \mathbf{v}.$$

From equation 2.3, we can deduce that the steady state is attained when the postsynaptic activity is equal to the total potential energy in the system. This also suggests that postsynaptic activity increases if it is less than the system's potential energy and decreases otherwise.

3 Allee Effect Postsynaptic Neuron Model and Motivation

Suppose that we have only one layer ($L = 1$) and a single postsynaptic neuron ($N_v = 1$). Therefore, $\mathbf{v} = v$ will be a scalar. Let us assume further that there is no recurrent connection ($\mathbf{Z} = \mathbf{0}$) and let $T(\mathbf{W}, \mathbf{0}, \mathbf{u}, \mathbf{v}) := T(\mathbf{W}, \mathbf{u}, v) = \mathbf{W}^T \cdot \mathbf{u}$. Per remark 3, $\mathbf{W}^T \cdot \mathbf{u}$ will be a scalar. Moreover, $\mathbf{W}$ is a

$1 \times N_u$ vector; thus, $\mathbf{W}^T \cdot \mathbf{W} = \|\mathbf{W}\|^2$ is a positive scalar. With the Hebbian rule and for $v = \mathbf{W}^T \cdot \mathbf{u}$, if we take the dot product on both sides of equation 2.2 by $2\mathbf{W}^T$, we will have

$$2\tau_{\mathbf{W}}\mathbf{W}^T \cdot \frac{d\mathbf{W}}{dt} = \tau_{\mathbf{W}} \frac{d\,\|\mathbf{W}\|^2}{dt} = 2v^2.$$

This shows that the Hebbian rule is dynamically unstable since synaptic weights will become unbounded over time. The same conclusion will be reached with the covariance rule. With the BCM rule, we have

$$\tau_{\mathbf{W}} \frac{d\,\|\mathbf{W}\|^2}{dt} = 2v^2(v - \theta_v).$$

This means that unbounded growth can be avoided by allowing θ_v to grow more rapidly than v at any instant. This is a rather stringent condition. Synaptic normalization amounts to imposing a global constraint to prevent unbounded growth. This is achieved with the Oja rule. Indeed, we will have

$$\tau_{\mathbf{W}} \frac{d\,\|\mathbf{W}\|^2}{dt} = 2v^2(1 - \alpha\,\|\mathbf{W}\|^2).$$

This shows that the growth rate of length of weights will be bounded over time by $\frac{1}{\alpha}$. For constants $A \geq 0$ and $K > 0$, consider the following plasticity rule:

$$\tau_{\mathbf{W}} \frac{d\mathbf{W}}{dt} = v\left(\mathbf{u} - \frac{v}{K}\mathbf{W}\right)\left(1 - \frac{A}{\|\mathbf{W}\|^2}\right). \tag{3.1}$$

We note also that when $A = 0$, equation 3.1 becomes the Oja rule with $\alpha = \frac{1}{K}$. Now multiplying both sides of this equation by $2\,\|\mathbf{W}\|^T$, we obtain

$$\frac{d\,\|\mathbf{W}\|^2}{dt} = 2v^2\left(1 - \frac{\|\mathbf{W}\|^2}{K}\right)\left(1 - \frac{A}{\|\mathbf{W}\|^2}\right). \tag{3.2}$$

In this case, the growth rate of length of weights is bounded above by $\max(A, K)$. Moreover, the threshold $\min(A, K)$ induces a strong Allee effect; that is, below this threshold, growth decreases to zero and above it increases. Another way of saying this is that this threshold induces a positive correlation between per capita growth rate $\frac{1}{\|\mathbf{W}\|^2}\frac{d\|\mathbf{W}\|^2}{dt}$ and $\|\mathbf{W}\|^2$ (see, for instance, Figure 3). We will therefore refer to such rules as the strong Allee effect plasticity rules.

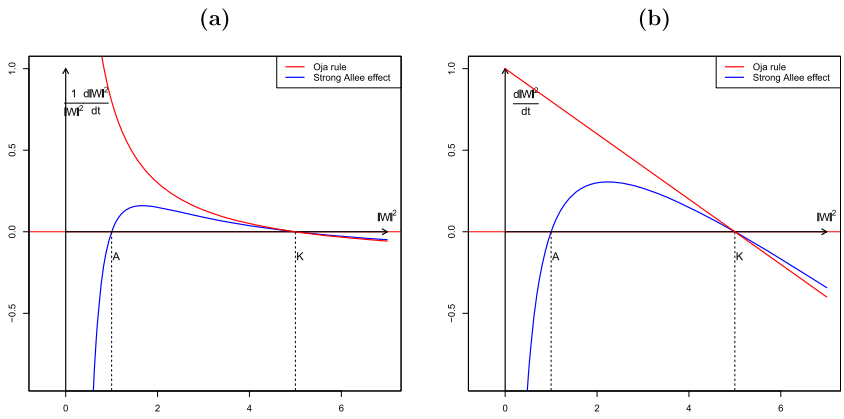

Figure 3: (a) The per capita growth rate of the length of weights is represented in the linear case for the Oja rule ($A = 0$) and the strong Allee effect rule ($A = 1$ and $K = 5$). For $A > 0$, we observe a local positive correlation between the per capita growth rate and the density $\|\mathbf{W}\|^2$ when $\|\mathbf{W}\|^2 < \mathbf{A}$ and a local negative correlation $\|\mathbf{W}\|^2 > \mathbf{A}$. In the Oja rule, the correlation is always negative, which means that there is no Allee effect. (b) The growth rate is represented. In the Oja rule, the bounded growth rate is required at lower lengths $\|\mathbf{W}\|^2$ to avoid blowup, which is not the case for the Allee rule.

In population dynamics in general, the term $\left(1 - A\,\|\mathbf{W}\|^{-2}\right)$ is used to account for the presence of sparse populations or mate limitation and enters the model multiplicatively. Adding this term as in equation 3.1 induces synaptic normalization in that when the weights are nonnegative, their growth is limited by the global threshold $\max(A, K)$. Moreover, convergence of $\|\mathbf{W}\|^2$ to $\max(A, K)$ induces competition between weights and preserves dynamic stability. A weak Allee effect may be introduced additively with a Holling's type II functional response term of the form $-\frac{m}{\|W\|^2+a}$, where a is referred to as an Allee constant and m is a mortality rate (see, for instance, Cai et al., 2012). However, the resulting plasticity rule blows up at lower values of $W(0)$. Another important observation is that with the strong Allee rule, the concept of strong or soft bounds can be considered; relative growth rate is used rather than growth as, for instance, in van Rossum and Barret (2012). In the sequel, we consider a strong Allee effect rule in more general settings.

Definition 3. *An Allee effect rule is a synaptic plasticity rule for which the relative growth rate (of the length of weights) has a positive correlation with the length of weights.*

Therefore, a strong Allee effect rule is a plasticity rule that has a threshold under which the length of weights decreases to zero and above which it increases to a dynamically stable point.

Definition 4. *Let* $\mathbf{W}$, $\mathbf{Z}$, $\mathbf{u}$, *and* $\mathbf{v}$ *be given as above. Consider an activity function* $T(\mathbf{W}, \mathbf{Z}, \mathbf{u}, \mathbf{v})$. *We define an Allee plasticity rule with nonplastic recurrent connections as the system of differential equations,*

$$\begin{cases} \tau_{\mathbf{W}} \dfrac{d\mathbf{W}}{dt} & = \mathbf{v}^T \left(\mathbf{u} - K^{-1}\mathbf{W}\mathbf{v}\right)\left(\mathbf{1} - A(\mathbf{W}^T\mathbf{W})^{-1}\right) \\ \tau_{\mathbf{v}} \dfrac{d\mathbf{v}}{dt} & = -\mathbf{v} + T(\mathbf{W}, \mathbf{Z}, \mathbf{u}, \mathbf{v}) \end{cases} . \tag{3.3}$$

Definition 5. *We define an Allee plasticity rule with plastic recurrent connections as the system of differential equations:*

$$\begin{cases} \tau_{\mathbf{W}} \dfrac{d\mathbf{W}}{dt} & = \mathbf{v}^T \left(\mathbf{u} - K^{-1}\mathbf{W}\mathbf{v}\right)\left(\mathbf{1} - A(\mathbf{W}^T\mathbf{W})^{-1}\right) \\ \tau_{\mathbf{v}} \dfrac{d\mathbf{v}}{dt} & = -\mathbf{v} + T(\mathbf{W}, \mathbf{Z}, \mathbf{u}, \mathbf{v}) \\ \tau_{\mathbf{Z}} \dfrac{d\mathbf{Z}}{dt} & = R(\mathbf{W}, \mathbf{Z}, \mathbf{u}, \mathbf{v}) \end{cases} . \tag{3.4}$$

where $R(\mathbf{W}, \mathbf{Z}, \mathbf{u}, \mathbf{v})$ *is the total recurrent (postsynaptic) activity and* $\tau_{\mathbf{Z}}$ *is a scaling constant.*

In the literature, two rules are often considered for $R(\mathbf{W}, \mathbf{Z}, \mathbf{u}, \mathbf{v})$. (See, for instance, Dayan and Abbott, 2001):

- Anti-Hebbian rule: $R(\mathbf{W}, \mathbf{Z}, \mathbf{u}, \mathbf{v}) = -\mathbf{v}^T\mathbf{v} + \beta\mathbf{Z}$, for some constant β.
- Goodall rule: $R(\mathbf{W}, \mathbf{Z}, \mathbf{u}, \mathbf{v}) = \mathbf{I} - (\mathbf{W}^{\mathbf{T}} \cdot \mathbf{u})\mathbf{v} - \mathbf{Z}$. This rule is often used because it produces decorrelated postsynaptic outputs and possesses homoskedasticity properties.

In the next sections, we provide a stability analysis of these plasticity rules.

4 Stability Analysis of a Single Postsynaptic Neuron Model

Here, we let $L = 1$ and $N_v = 1$. In the presence of a single postsynaptic neuron, the matrix $\mathbf{v}$ is reduced to a constant v, and the recurrent connection matrix $\mathbf{Z}$ is reduced to a single constant z. There are two cases to consider. First, there could be no recurrent connection between v and itself ($z = 0$) (see Figure 4a). Second, there could be a recurrent connection with weight $z \neq 0$ (see Figure 4b).

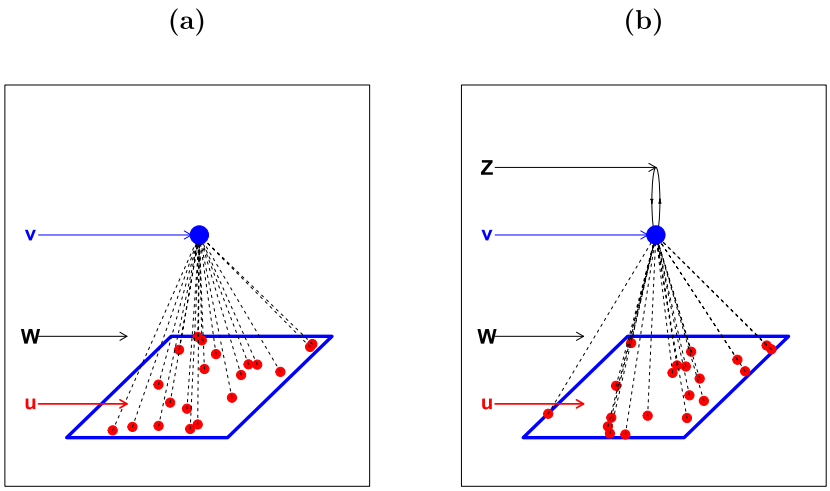

Figure 4: (a) One postsynaptic neuron with no recurrent connection. (b) One postsynaptic neuron with one recurrent connection.

4.1 Single Postsynaptic Neuron with No Recurrent Connection. In this case, we will have $\mathbf{Z} = 0$ and $\mathbf{v} = v$. Consider the Allee-type system given by

$$\begin{cases} \tau_{\mathbf{W}} \dfrac{d\,\|\mathbf{W}\|^2}{dt} & = 2v\left(T_1(\mathbf{W},\mathbf{u}) - \dfrac{v}{K}\|\mathbf{W}\|^2\right)\left(1 - \dfrac{A}{\|\mathbf{W}\|^2}\right) \\ \tau_v \dfrac{dv}{dt} & = -v + T_2(\mathbf{W},\mathbf{u}) \end{cases}. \tag{4.1}$$

We will use the notation $x =: \|\mathbf{W}\|^2$, $y := v$, $u = \|\mathbf{u}\|\cos(\theta)$, where θ is the angle between the vector $\mathbf{W}$ and $\mathbf{u}$. Since $\mathbf{W}^T \cdot \mathbf{u} = \|\mathbf{W}\|\,\|\mathbf{u}\|\cos(\theta)$, in the linear case, we will have $T_1(\mathbf{W},\mathbf{u}) = T_2(\mathbf{W},\mathbf{u}) = \mathbf{W}^T \cdot \mathbf{u} = u\sqrt{x}$. In this case for $x > 0$, we would have the system

$$\begin{cases} \tau_x \dfrac{dx}{dt} & = g_1(x,y) := 2y\left(u\sqrt{x} - \frac{yx}{K}\right)\left(1 - \frac{A}{x}\right) \\ \tau_y \dfrac{dy}{dt} & = g_2(x,y) := -y + u\sqrt{x} \end{cases}. \tag{4.2}$$

The x-isocline is given by the equations $y = 0$, $uK\sqrt{x} = yx$, and $x = A$ and the y-isocline is given by $y = u\sqrt{x}$. The steady states of this system are $(x, 0)$, $(K, u\sqrt{K})$, and $(A, u\sqrt{A})$. We now discuss their stability.

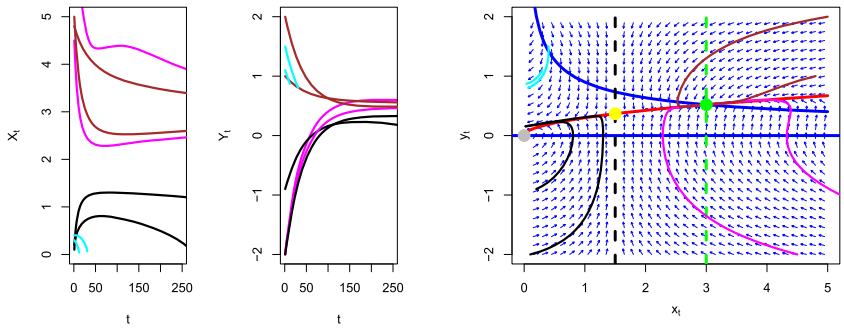

Figure 5: Time series and phase space diagram when $A = 1.5$ and $K = 3$. The point $(A, u\sqrt{A})$ is unstable, and $(K, u\sqrt{K})$ is stable.

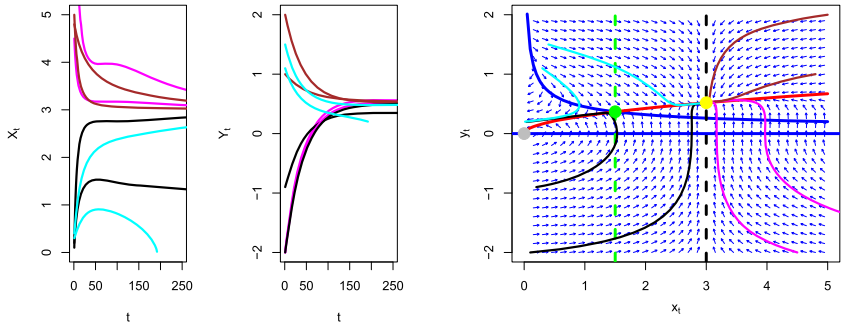

Figure 6: Time series and phase space diagram when $A = 3$ and $K = 1.5$. The point $(A, u\sqrt{A})$ is stable, and $(K, u\sqrt{K})$ is unstable.

Theorem 1. *In the system (see equation 4.2):*

(i) For fixed $x > 0$, the equilibrium point $(x, 0)$, is an attractor.
(ii) If $K < A$, then $(A, u\sqrt{A})$ is asymptotically stable and $(K, u\sqrt{K})$ is unstable.
(iii) If $A < K$, then $(A, u\sqrt{A})$ is unstable and $(K, u\sqrt{K})$ is asymptotically stable.
(iv) If $K = A$, then $(K, u\sqrt{K})$ is an attractive line of equilibria.

Remark 4.

(a) We note that the classification of a steady state is independent of the sign of u because Δ, $tr(J)$, and $det(J)$ all depend on u^2.
(b) We note, however, that $T_2(\mathbf{W}, \mathbf{u})$ needs not be a linear function of $\mathbf{W}$ and $\mathbf{u}$. Dynamically, their behaviors are similar, especially when $T_2(\mathbf{W}, \mathbf{u}) = \mathbf{W}^T \cdot G(\mathbf{u})$ for some nonlinear function G.

In Figures 5 to 9, we illustrate the above results by plotting the time series of x_t and y_t, for $t = 0, \ldots, 250$. We let A and K take interchangeably the values

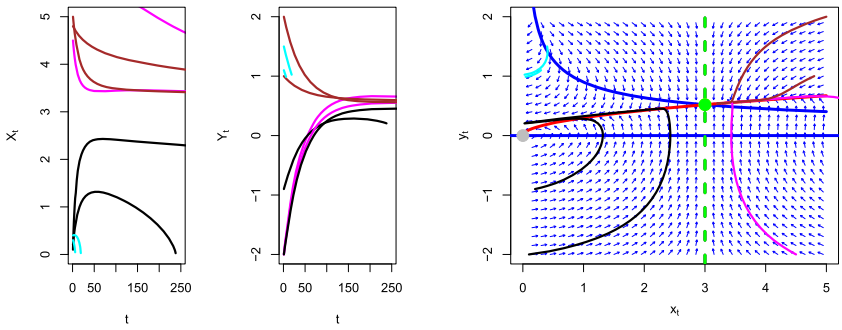

Figure 7: Time series and phase space diagram when $A = K = 3$. The point $(A, u\sqrt{A}) = (K, u\sqrt{K})$ is a saddle.

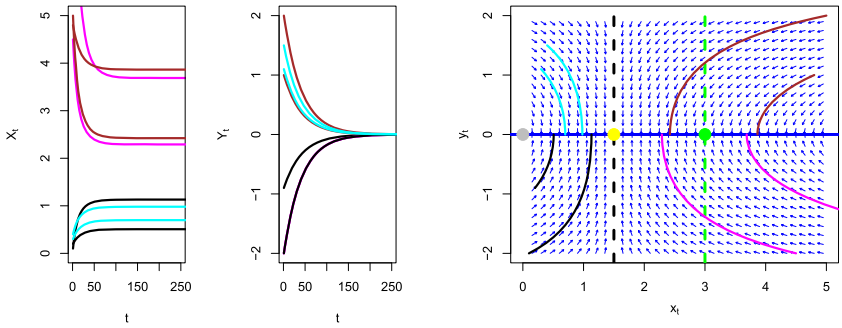

Figure 8: Time series and phase space diagram when $A = 1.5$, $K = 3$, and $u = 0$. In this case, every point $(x, 0)$ is an attractor.

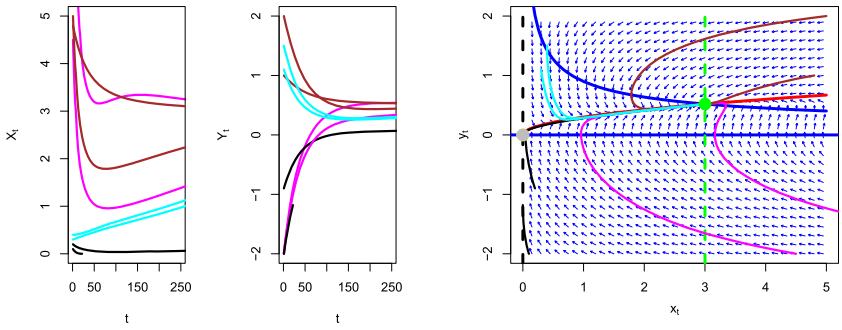

Figure 9: Time series and phase space diagram when $A = 0$ and $K = 3$. This is the Oja rule, and the point $(K, u\sqrt{K})$ is stable.

1.5 and 3 in Figures 5, 6, and 8. The starting points of the trajectories are $(0.1, -2)$, $(0.2, -0.9)$ in black, $(0.3, 1.1)$, $(0.4, 1.5)$ in cyan, $(4.8, 1)$, $(5, 2)$ in brown, and $(9.8, -2)$, $(4.5, -2)$ in magenta. In Figures 5, 6, 7, and 9, we take without loss of generality $u = 0.3$. The solid blue curve represents the x-isocline given as $y = \frac{uK}{\sqrt{x}}$. The solid blue line represents the x-isocline $y = 0$, and the solid red curve represents the y-isocline given as $y = u\sqrt{x}$. The dots are the intersection between the x- and y-isoclines. In particular, the gray dot represents the origin $(0, 0)$, and the yellow dot has coordinates $(A, u\sqrt{A})$, and is the intersection between the x-isocline $x = A$ and the y-isocline $y = u\sqrt{x}$. Likewise, the green dot is the intersection between the x-isocline $x = K$ and the y-isocline $y = u\sqrt{x}$ with coordinates $(K, u\sqrt{K})$. From these figures, we confirm the results above in that $(A, u\sqrt{A})$ and $(K, u\sqrt{K})$ are either attractors or saddle points. Figure 8 confirms that when $u = 0$, the line $y = 0$ is a sink.

4.2 Discussion. In the case of one neuron with nonplastic recurrent connection, establishing stability of the steady states is relatively manageable compared to the case of a plastic connection. Figure 5 is similar to a typical case in ecology where the Allee threshold A is less than K. We clearly see that in the region below A, trajectories of synaptic weights converge to zero, while trajectories of postsynaptic neurons may be in either excitatory or inhibitory states. Interestingly, excitatory postsynaptic neurons never become inhibitory since they never cross the red curve. In that same region, inhibitory neurons become excitatory over time but with decreasing synaptic weights. Figure 6 shows that if $A > K$, the Allee effect is no more guaranteed to occur below A or even below K. In fact, some neurons, whether in excitatory or inhibitory states, would have decaying or increasing synaptic weights. This is the case for the trajectories in black and cyan. Figure 7 is the case when $A = K$ and there is an Allee effect. Figure 8 is an illustration of the situation where at some point in time, there is no presynaptic activity. Since postsynapatic is already in excitatory or inhibitory modes, they will decay to zero rather quickly. Figure 9 is essentially the Oja rule, and there is no Allee effect.

4.3 Single Postsynaptic Neuron with One Constant Recurrent Connection. In this case, $\mathbf{Z} = z$ and $\mathbf{v} = v$ are constant with $\frac{d\mathbf{Z}}{dt} = 0$. As we observe above, we consider the system given by

$$\begin{cases} \tau_{\mathbf{W}} \frac{d\|\mathbf{W}\|^2}{dt} &= 2v\left(\mathbf{W}^T \cdot \mathbf{u} - \frac{v}{K}\|\mathbf{W}\|^2\right)\left(1 - \frac{A}{\|\mathbf{W}\|^2}\right) \\ \tau_v \dfrac{dv}{dt} &= -v + T_2(\mathbf{W}, \mathbf{u}, z, v) \end{cases}. \tag{4.3}$$

Using the notation $x =: \|\mathbf{W}\|^2$, $y := v$, $u = \|\mathbf{u}\|\cos(\theta)$, and given functions $f_1(x, u)$ and $f_2(x, y, u, v)$, this system is of the form

$$\begin{cases} \tau_x \dfrac{dx}{dt} & = g_1(x,y) := 2y\left(f_1(x,u) - \frac{yx}{K}\right)\left(1 - \frac{A}{x}\right) \\ \tau_y \dfrac{dy}{dt} & = g_2(x,y) := -y + f_2(x,y,u,z) \end{cases}. \tag{4.4}$$

This system has similar dynamics to that of system 4.2. In the linear case where $f_2(x,y,u,z) = u\sqrt{x} + zy$, $\frac{dy}{dt} = (z-1)y + u\sqrt{x} = 0$ if $(1-z)y = u\sqrt{x}$. For $z = 0$, this is the parabola (red solid curve) obtained in the previous case. When z approaches 1, this parabola becomes increasingly "steeped" and eventually explodes into the y-axis when $z = 1$. In the latter case, there is no steady state in the system since they are always given as intersections between the parabola and the vertical lines $x = A$ and $x = (1-z)K$. In reality, there will be infinitely many points of intersection between the parabola and the vertical lines.

4.4 Single Postsynaptic Neuron with One Plastic Recurrent Connection. For a single postsynaptic neuron with one plastic recurrent connection, we will have $\mathbf{Z} = z$ and $\mathbf{v} = v$. In this letter, we use Goodall's rule for its decorrelation properties. For a single neuron, we consider the system given by

$$\begin{cases} \tau_{\mathbf{W}} \frac{d\|\mathbf{W}\|^2}{dt} & = 2v\left(\mathbf{W}^T \cdot \mathbf{u} - \frac{v}{K}\|\mathbf{W}\|^2\right)\left(1 - \frac{A}{\|\mathbf{W}\|^2}\right) \\ \tau_v \dfrac{dv}{dt} & = -v + T_2(\mathbf{W}, \mathbf{u}, z, v) \\ \tau_z \dfrac{dz}{dt} & = -(\mathbf{W}^T \cdot \mathbf{u})v + 1 - z \end{cases}. \tag{4.5}$$

We now discuss the steady states of the system above (see Table 10).

Case 1: $v = 0$. Then we would have $T_2(\mathbf{W}, \mathbf{u}, z, v) = 0$, which, as above, can only happen if $u = 0$ and $v = 0$. In this case, the third equation suggests that we must have $z = 1$. Thus, in the space formed by $x = \|\mathbf{W}\|^2, y = v$, and z, the line parallel to the x-axis with equation $y = 0, z = 1$ is a steady state.

Case 2: $v \neq 0, \mathbf{W}^T \cdot \mathbf{u} = \frac{v}{K}\|\mathbf{W}\|^2$. This condition is equivalent to $v = \frac{K(\mathbf{W}^T \cdot \mathbf{u})}{\|\mathbf{W}\|^2}$. From the second equation in equation 4.5, we have $v = \mathbf{W}^T \cdot \mathbf{u} + zv$; therefore, we deduce that $z = 1 - \frac{\|\mathbf{W}\|^2}{K}$. Using the third equation $-(\mathbf{W}^T \cdot \mathbf{u})v + 1 - z = 0$, it follows that $z = 1 - \frac{\|\mathbf{W}\|^2}{K}v^2$. Since the values of z must be the same, it follows that we should have $v^2 = 1$. The latter entails having $\|\mathbf{W}\|^2 = K\left|\mathbf{W}^T \cdot \mathbf{u}\right|$ and $z = 1 - \left|\mathbf{W}^T \cdot \mathbf{u}\right|$. We conclude that there are two steady states in the space formed by $x = \|\mathbf{W}\|^2, y = v$, and z, namely, the lines

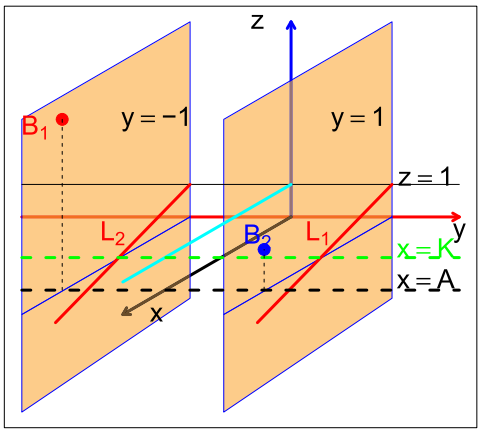

Figure 10: Steady states (in red) of system 4.5, when $A > K$.

$$L_1 : z = 1 - \frac{x}{K}, \quad y = 1,$$
$$L_2 : z = 1 - \frac{x}{K}, \quad y = -1.$$

Case 3: $v \neq 0$, $\|\mathbf{W}\|^2 = A$. In this case, $v = \mathbf{W}^T \cdot \mathbf{u} + zv$ and thus $v = \frac{\mathbf{W}^T \cdot \mathbf{u}}{1-z}$. We note from above that if $v \neq 0$, then $z \neq 1$. It follows from the third equation of the system 4.5 that $z = 1 - (\mathbf{W}^T \cdot \mathbf{u})v$, and therefore we can deduce that $(1-z)(1-v^2) = 0$. Since $z \neq 1$, we must have $v^2 = 1$. The latter implies that $\left|\mathbf{W}^T \cdot \mathbf{u}\right| = |1-z|$. Thus, $z = 1 \pm \mathbf{W}^T \cdot \mathbf{u}$. We conclude that there are two steady states in the space formed by $x = \|\mathbf{W}\|^2$, $y = v$, and z, namely, the points

$$B_1 = (A, -1, 1 + u\sqrt{A}), \quad B_2 = (A, 1, 1 - u\sqrt{A}).$$

Using the notation $x =: \|\mathbf{W}\|^2$, $y := v$, $u = \|\mathbf{u}\| \cos(\theta)$, and for given functions $f_1(x,u)$ and $f_2(x,y,z,u)$, system 4.5 is of the form

$$\begin{cases} \tau_x \dfrac{dx}{dt} & = g_1(x,y,z) := 2y\left(f_1(x,u) - \frac{yx}{K}\right)\left(1 - \frac{A}{x}\right) \\ \tau_y \dfrac{dy}{dt} & = g_2(x,y,z) := -y + f_2(x,y,z,u) \\ \tau_z \dfrac{dz}{dt} & = g_3(x,y,z) := f_3(x,y,u) + 1 - z \end{cases} . \tag{4.6}$$

Our first result in this section concerns the stability of the steady state line $x > 0, y = 0, z = 1$ and the points B_1 and B_2.

Theorem 2. *Consider the system 4.6, where* $f_1(x,u) = u\sqrt{x}$, $f_2(x,y,z,u) = u\sqrt{x} + zy$, *and* $f_3(x,y,u) = -uy\sqrt{x}$.

(i) *If* $u = 0$, *then the steady state is the line* $(x,0,1)$ *for* $x > 0$ *and it is always stable.*
(ii) *Suppose* $u > 0$.
  (a) *If* $u < \frac{2\sqrt{A}}{K}$, *then* B_1 *is unstable and* B_2 *is stable.*
  (b) *If* $u > \frac{2\sqrt{A}}{K}$, *then* B_1 *and* B_2 *are unstable.*
(iii) *Suppose* $u < 0$.
  (a) *If* $-2\sqrt{A}\max\{2A, K\} \leq u$, *then* B_1 *and* B_2 *are stable.*
  (b) *If* $u < -2\sqrt{A}\max\{2A, K\}$, *then* B_1 *and* B_2 *are unstable.*
  (c) *If* $-2\sqrt{A}\min\{2A, K\} < u < -2\sqrt{A}\max\{2A, K\}$, *one of* B_1 *or* B_2 *is unstable and the other is stable.*

The proof is in the appendix. Our second result discusses the stability of the steady states L_1 and L_2.

Theorem 3. *Consider the system 4.6, where* $f_1(x,u) = u\sqrt{x}$, $f_2(x,y,z,u) = u\sqrt{x} + zy$, *and* $f_3(x,y,u) = -uy\sqrt{x}$. *Put*

$$\alpha_1 = 2\left(\frac{u}{2\sqrt{x}} - \frac{1}{K}\right)\left(1 - \frac{1}{A}\right) + 2\left(u\sqrt{x} - \frac{2x}{K}\right)\left(\frac{A}{x^2}\right),$$

$$\alpha_2 = \left(2u\sqrt{x} - \frac{4x}{K}\right)\left(1 - \frac{A}{x}\right), \qquad \alpha_3 = 0,$$

$$\beta_1 = \frac{u}{2\sqrt{x}}, \qquad \beta_2 = -\frac{x}{K}, \qquad \beta_3 = -1,$$

$$\gamma_1 = \frac{u}{2\sqrt{x}}, \qquad \gamma_2 = -u\sqrt{x}, \qquad \gamma_3 = -1.$$

In addition, we let

$$a_2 = (\alpha_1 + \beta_2 - 1),$$

$$a_1 = \alpha_1(1 - \beta_2) + \beta_2 - \gamma_2 + \alpha_2\beta_1,$$

$$a_0 = \alpha_1(\gamma_2 - \beta_2).$$

(i) *Suppose* $a_0 = 0$.
  (a) *If* $a_2^2 + 4a_1 < 0$ *and* $a_2 < 0$, *then* L_1 *and* L_2 *are stable.*
  (b) *Suppose* $a_2^2 + 4a_1 > 0$.
    1. *If* $a_1 > 0$ *and* $a_2 > 0$, *then* L_1 *and* L_2 *are unstable.*
    2. *If* $a_1 < 0$ *and* $a_2 > 0$, *then* L_1 *and* L_2 *are stable.*
    3. *If* $a_1 > 0$ *and* $a_2 < 0$ *or* $a_1 < 0$ *and* $a_2 > 0$, *then* L_1 *and* L_2 *are unstable.*

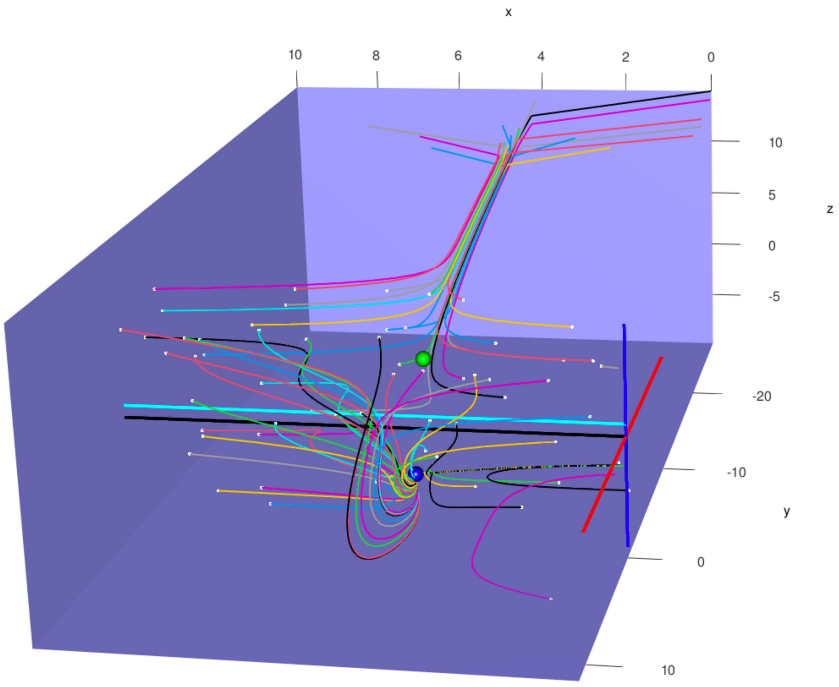

Figure 11: Illustration of the dynamics of the system above for $u = 2, K = 1$, and $A = 4$. $u < \frac{2\sqrt{A}}{K}$, and we observe that B_2 is stable and B_1 is unstable. The cubes $R_1 = [0, 4] \times [0, 10] \times [-5, 0]$ and $R_2 = [0, 4] \times [-20, 0] \times [-5, 10]$ are the Allee regions. Starting trajectories will eventually converge to 0 in x, leading to absence of plasticity.

(iii) If $a_0 > 0, a_1, a_2$, and $a_1 a_2 > a_1$, then L_1 and L_2 are stable, otherwise, they are unstable.

The proof is in the appendix.

4.5 Illustration. Since they are many cases to consider, we only illustrate a couple of them for simplicity. In Figures 11 to 13, we show the dynamics of system 4.5. We choose $M = 20$ different trajectories with length $N = 5000$. The initial states are chosen randomly. Since $x = \|\mathbf{W}\|^2$ must be positive, we randomly select M starting points x_0 in the interval (0, 5). The starting values y_0 are chosen randomly as $M/2 = 10$ in the interval $(-5, 0)$ and $M/2 = 10$ in $(0, 5)$. The starting values z_0 are chosen randomly as $M/2 = 10$ in the interval $(-10, 0)$ and $M/2 = 10$ in $(0, 10)$. The starting points (x_0, y_0, z_0) are the white dots in the figures that follow. The green sphere is B_1 and the blue sphere is B_2.

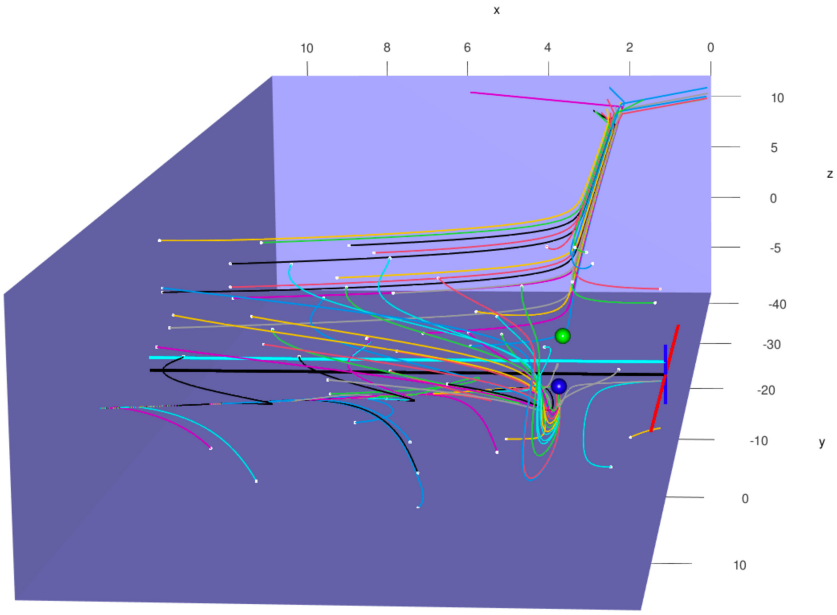

Figure 12: Illustration of the dynamics of the system above for $u = 1.1$, $K = 3$, and $A = 2$. $u > \frac{2\sqrt{A}}{K}$, and we observe that B_1 and B_2 are unstable. In fact, B_1 is clearly a repeller point, whereas B_1 is a saddle point. This case is less realistic since synaptic normalization is never achieved. In fact, the lengths of weights x increase without bound, while the postsynaptic activities y, though different at early times, become increasingly similar over time (straight line). The Allee regions are the cubes $R_1 = [0, 2] \times [0, 10] \times [-5, 0]$ and $R_2 = [0, 2] \times [-40, 0] \times [-5, 10]$. We observe that the gray trajectory starting just above R_1 does not converge to zero because it gets into the basin of attraction of L_2 and increases thereafter.

4.6 Discussion. The first simulation shows that the trajectories of the lengths of weights x decrease to either $A = 4$ or 0. The second simulation is more nuanced in that some trajectories decrease to $A = 2$ first. Then, after a while, they either decrease to 0 or increase. Other trajectories will first increase and then decrease to 0. Finally, some will increase without bound after initially decreasing to close to $A = 2$. What these simulations show is that the size of the Allee region (region where the Allee effect occurs) depends on the value of A. Clearly, if $A = 0$, there is no Allee region and the model is reduced to the Oja rule. An important observation is that the fixed points B_1 and B_2 both depend on A. The first simulation shows that if $A = 0$ (Oja rule), then weight lengths x all decrease to 0, without any possibility of recovering. This means that our system, while stable in the long term, represents a drift toward an absence of plasticity. In a sense, the parameter

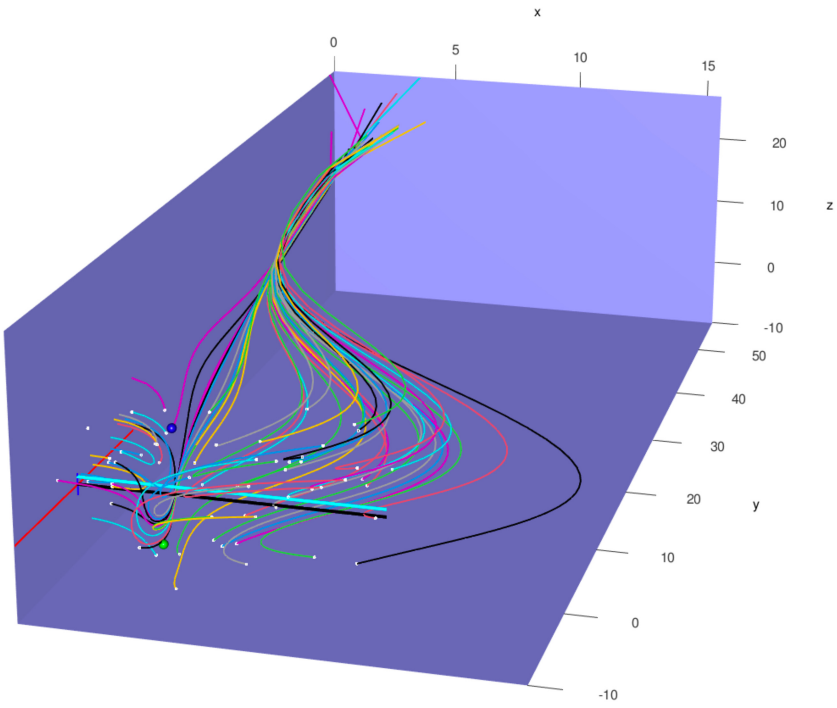

Figure 13: Illustration of the dynamics of the system above for $u = -4$, $K = 4$, and $A = 4$. $u > -2\sqrt{A}\max\{2A, K\}$, and we observe that B_1 and B_2 are unstable. This case is less realistic since synaptic normalization is not achieved all the time. Moreover, postsynaptic activities y and recurrent connections z increase without any bound. If we look closely at B_1 and B_2, we clearly see that no trajectory converges to B_1 and B_2. The Allee region is cube $R_1 = [0, 4] \times [0, 50] \times [-10, 20]$.

A must be positive if we want to have more than a drift toward the absence of plasticity for all trajectories.

From above, we clearly see that there is an advantage to studying the length of weights rather than individual weights. The complexity of the dynamics is vastly reduced. This approach makes studying large numbers of layers mathematically possible while maintaining interpretability of the results. The main drawback, as illustrated by the results above (see theorems 2 and 3) is that stability analysis, while feasible, still depends unfortunately on complicated quantities.

5 Model of Multiple Postsynaptic Neurons

In the single postsynaptic neuron model, we did not include recurrent connections. For a multiple postsynaptic model, we have to consider recurrent

connections that themselves may be fixed or plastic. Another important aspect to consider is that of a layered system where pre- and postsynaptic neurons are on different layers. It is entirely possible that this aspect may help reduce redundancies and correlations among output units.

5.1 Multiple Output Units with Constant Recurrent Connections. In this case, $\mathbf{Z}$ and $\mathbf{v}$ are nonzero matrices with $\mathbf{Z}$ constant over time. We fix $1 \le \ell \le L$ and $1 \le j \le N_v$. The assumption here is still that we have N_u presynaptic neurons and N_v postsynaptic neurons per layer. Now we let $\mathbf{W}_j^{(\ell)}$ be $1 \times N_u$ vector of synaptic weights from the N_u presynaptic neurons $\mathbf{u}^{(\ell)}$ on the ℓth layer to the jth postsynaptic neurons $v_j^{(\ell)}$ on the ℓth layer. In this case, equation 4.3 becomes

$$\begin{cases} \tau_{\mathbf{W}_j^{(\ell)}} \dfrac{d\left\|\mathbf{W}_j^{(\ell)}\right\|^2}{dt} & = 2v_j^{(\ell)}\left([\mathbf{W}_j^{(\ell)}]^T \cdot \mathbf{u}^{(\ell)} - \dfrac{v_j^{(\ell)}}{K_j^{(\ell)}}\left\|\mathbf{W}_j^{(\ell)}\right\|^2\right)\left(1 - \dfrac{A_j^{(\ell)}}{\left\|\mathbf{W}_j^{(\ell)}\right\|^2}\right). \\ \tau_{v_j^{(\ell)}} \dfrac{dv_j^{(\ell)}}{dt} & = -v_j^{(\ell)} + T\left(\mathbf{W}_j^{(\ell)}, \mathbf{u}^{(\ell)}, z_j^{(\ell)}, v_j^{(\ell)}\right) \end{cases} \tag{5.1}$$

We see that for these given ℓ and j, system 5.1 has similar dynamics as system is 4.3. However, there are other considerations to account for in this case. The system's parameters all depend on ℓ and j. The assumptions that timescale constants $\tau_{\mathbf{W}_j^{(\ell)}}$ are the same is not completely unrealistic, especially if the system evolves in a homogeneous ambient space. The same can be said of timescale constants $\tau_{v_j^{(\ell)}}$. The thresholds $A^{(\ell)}$ and $K^{(\ell)}$ can be the same or can vary, selected according to a chosen distribution. In the constant case, the dynamics of system 5.1 is identical across all layers; thus, the postsynaptic neurons will be perfectly correlated. In the case where these thresholds are not identical, of interest is understanding how and if the threshold vectors $\boldsymbol{A}^{(\ell)} = (A_j^{(\ell)})$ and $\boldsymbol{K}^{(\ell)} = (K_j^{(\ell)})$ for $1 \le j \le N_v, 1 \le \ell \le L$ affect the correlation between postsynaptic neurons $\mathbf{v}^{(\ell)}$ per layer.

To illustrate the potential effect of thresholds, we select $N_v = 150$ samples of K from a truncated normal distribution $N(\mu = 0, \sigma^2 = 100)$ over an interval [1.5, 30]. Likewise, we will select N_v samples A from an exponential distribution $\exp(\theta = 0.5)$. These distributions are different enough to discriminate the potential effect of thresholds A and K. The lengths of the synaptic weights $x = \|\mathbf{W}\|^2$ will be initialized uniformly over the interval $(0, 5)$. We fix the presynaptic length $u = 0.3$ and let $z_j^{(\ell)} = 0.4$. The postsynaptic values v will be initialized uniformly within the interval $[-2, 2]$. We will observe the N_v trajectories of v from $t = 0$ to $t = 25$ because not all of them will converge. In fact, for given N_v postsynaptic neurons, only an $N_v^* \le N_v$

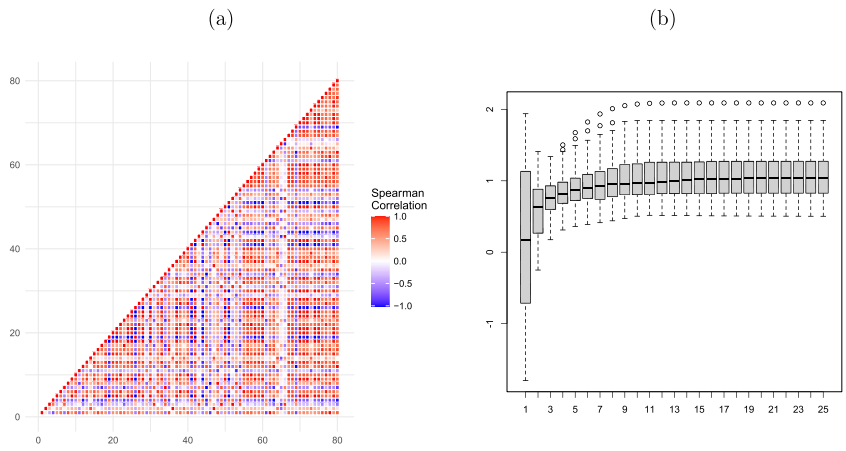

Figure 14: (a) Heat map showing the correlation between the $N_v^* = 80$ convergent trajectories. (b) Box plots showing the evolution of the distribution of trajectories form time $t = 1$ to $t = 25$.

will converge. We will therefore assess the correlation between these N_v^* trajectories. In Figure 14a, the heat map shows that the majority of the $N_v^* = 80$ postsynaptic neurons v are highly correlated. Some of them, albeit a small number, are decorrelated. It could be due to the randomness in the choice of the parameters above, or it could be due to the fact that the model itself reduces correlation, without any formal decorrelation mechanism like Goodall's. The box plots in Figure 14b show the evolution of the N_v^* trajectories over time. While the distribution of the $N_v^* = 80$ trajectories differs significantly initially, they become increasingly similar over time, despite a few outliers. It also shows that the variance of outputs is constant over time.

To ascertain whether the number of decorrelated postsynaptic neuron v is independent of the number N_v chosen, we introduce the decorrelation percentage. There are $\binom{N_v^*}{2}$ Spearman correlation coefficients. The decorrelation percentage is the proportion of these coefficients less than 0.2 (considered a weak correlation in the literature). Figure 15 shows that the decorrelation percentage is high when N_v is low and decreases with increasing N_v.

5.2 Multiple Output Units with Plastic Recurrent Connections. In this case, $\mathbf{Z}$ and $\mathbf{v}$ are matrices where $\mathbf{Z}$ is time dependent. As in section 5.1, we fix $1 \leq k, \ell \leq L$ and $1 \leq j, m \leq N_v$. Let $z_{mj}^{(k,\ell)}$ represent the plastic weight connecting the jth postsynaptic neuron $v_j^{(\ell)}$ on the ℓth layer with the mth postsynaptic neuron $v_m^{(k)}$ on the kth layer. System becomes

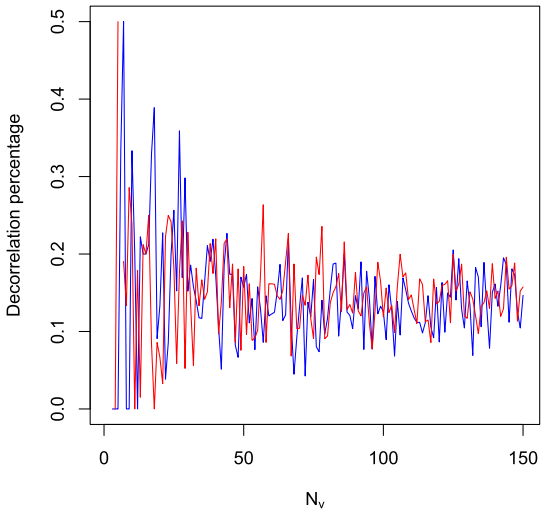

Figure 15: Decorrelation percentage for the Oja model (red) and the Allee model (blue), both as functions of the number of postsynaptic neurons per layers N_v.

$$\begin{cases} \tau_{\mathbf{W}_j^{(\ell)}} \dfrac{d\left\|\mathbf{W}_j^{(\ell)}\right\|^2}{dt} & = 2v_j^{(\ell)} \left([\mathbf{W}_j^{(\ell)}]^T \cdot \mathbf{u}^{(\ell)} - \dfrac{v_j^{(\ell)}}{K_j^{(\ell)}} \left\|\mathbf{W}_j^{(\ell)}\right\|^2 \right) \left(1 - \dfrac{A_j^{(\ell)}}{\left\|\mathbf{W}_j^{(\ell)}\right\|^2} \right) \\ \tau_{v_j^{(\ell)}} \dfrac{dv_j^{(\ell)}}{dt} & = -v_j^{(\ell)} + T\left(\mathbf{W}_j^{(\ell)}, \mathbf{u}^{(\ell)}, z_{mj}^{(k,\ell)}, v_j^{(\ell)}\right) \\ \tau_{z_{mj}^{(k,\ell)}} \dfrac{dz_{mj}^{(k,\ell)}}{dt} & = -\left([\mathbf{W}_j^{(\ell)}]^T \cdot \mathbf{u}^{(\ell)} \right) v_j^{(\ell)} + 1 - z_{mj}^{(k,\ell)} \end{cases} . \tag{5.2}$$

As above, we may assume that the ambient space is homogeneous so that timescale constants $\tau_{z_{mj}^{(k,\ell)}}$ are the same. To obtain Figure 16, we used the same parameters as in section 5, with the addition of plastic recurrent connections. The heat map in Figure 16a, shows that the $N_v^* = 107$ postsynaptic neurons are less correlated than in the previous case above based on the prevalence of light red and light blue. Figure 16b shows that the distribution of the trajectories stabilizes relatively quickly compared to the case above (see Figure 17).

5.3 Discussion. From the simulations above, we can draw a few observations:

(a) (b)

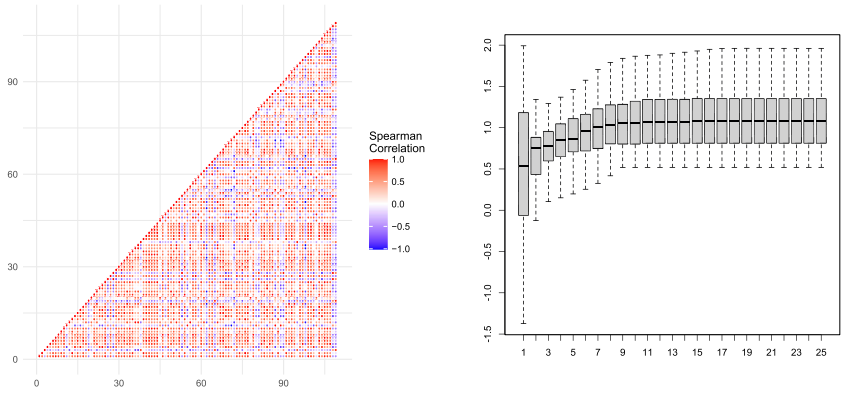

Figure 16: (a) Heat map showing correlation between the $N_v^* = 107$ convergent trajectories. (b) Box plots showing the evolution of the distribution of trajectories from time $t = 1$ to $t = 25$.

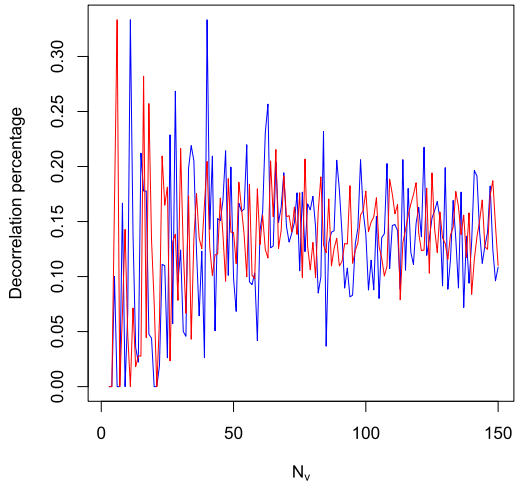

Figure 17: Decorrelation percentage for the Oja model (red) and the Allee model (blue), both as functions of the number of postsynaptic neurons per layers N_v.

1. The presence of the Allee effect term $(1 - A\,\|\mathbf{W}\|^{-2})$ in the model overall increases decorrelation, relatively speaking (see Figure 15). Decorrelation is even increased when coupled with a decorrelation mechanism such as Goodall's method.

2. We selected thresholds A and K randomly from noisy distributions so that any measured effects would be independent of their selection. Another important observation is that the initialization of v and $\mathbf{Z}$ does not seems to produce similar results as seen above, even when choosing from heavy-tailed distributions like $N(0, 10)$ or a Student-t with low degrees of freedom.
3. Systems 5.1 and 5.2 are discussed in the context where the timescales are identical per layer. However, if they are chosen to be different and large, then the output units become highly correlated, within layers, reversing the decorrelation gains an Allee term would bring.
4. It seems as though the model, as written in equations 5.1 and 5.2, may be local to a single chosen layer. However, it is hardly the case given that one can consider that each layer has a single postsynaptic neuron, similar to discrete dynamics of dynamic neural fields (see Kwessi, 2021b).

6 Conclusion

In this letter, we have proposed a definition of the Allee effect in neuroplasticity that maintains the spirit of the Allee effect as originally proposed by Allee (1949). We have also proposed a learning rule that is more general than the Oja learning rule while preserving multiplication normalization, controlling for unbounded growth, and inducing competition between weights. The model in its matrix form has the advantage that it can accommodate single or multiple pre- and postsynaptic neurons, with and and without recurrent connections. Stability analysis was discussed with simulations to illustrate results. Absence of plasticity in the brain can be due to many factors and can be observed in many brain pathologies such as Alzheimer's, Parkinson's, and Huntington's diseases and stroke. Using the firing-rate equation to model postsynaptic activities could be a limiting factor in the model in that diffusion is not accounted for. A further improvement involving a diffusion term or a lattice differential equation would probably add more nuance and could be worthwhile. In ecology, remedies to an Allee effect such as immigration have been proposed in Assas et al. (2015b), together with mathematical models explaining the process. This amounts in practice to adding either new offsprings from different population patches or to controlling predation. In the brain, however, it is not clear how one would go about this. Often neuroscientists focus on reactivating lost or dormant neurotransmitters by using new technologies such as brain implants. While applications of these implants have been numerous, mathematical models have lagged or, at best, have been an adaptation or a reduction of the Hogkin-Huxley model (Drapaca, 2018). The model we proposed is different and is sensitive to external inputs (as in an Allee-type model) and thus could be used to model the effects of brain implants. From a dynamical systems point of view, the model we propose is

complex enough to accommodate a complex structure like the brain. Simulations do show that there are enough parameters in the model to capture a variety of phenomena related to neuroplasticity. From a mathematical point of view, studying the length of weights (rather than individual weights) coupled with other numerical quantities such as postsynaptic signals and their strengths reduces the complexity of the problem while maintaining interpretability of the results. From a purely scientific point of view, the model offers to merge some notions discussed in ecology and neuroscience, and it shows that these seemingly isolated areas from each other actually have some similarities.

Appendix A: Stability Analysis of System 4.2

The partial derivatives of g_1 and g_2 in system 4.2 are:

$$\frac{\partial g_1(x,y)}{\partial x} = 2y\left(\frac{u}{2\sqrt{x}} - \frac{y}{K}\right)\left(1 - \frac{A}{x}\right) + 2y\left(u\sqrt{x} - \frac{yx}{K}\right)\left(\frac{A}{x^2}\right),$$
$$\frac{\partial g_1(x,y)}{\partial y} = \left(2u\sqrt{x} - 4\frac{yx}{K}\right)\left(1 - \frac{A}{x}\right),$$
$$\frac{\partial g_2(x,y)}{\partial x} = \frac{u}{2\sqrt{x}},$$
$$\frac{\partial g_2(x,y)}{\partial y} = -1.$$

A.1 Stability Analysis of Steady States $(x, 0)$**.** Since, per remark 2, $y = 0$ if and only if $u = 0$, the Jacobian matrix $J(x, 0)$ at $(x, 0)$ of the system is given as

$$J(x,0) = \begin{pmatrix} 0 & 0 \\ 0 & -1 \end{pmatrix}.$$

The eigenvalues are therefore $\lambda_1 = 0$ and $\lambda_2 = -1$. The trajectories in the eigenspace of $\lambda_1 = 0$ are time independent, so this eigenspace is a line of equilibria, whereas the trajectories decay to 0 along the eigenspace of $\lambda_2 < 0$. So the point $(x, 0)$ is stable but not asymptotically stable.

A.2 Stability Analysis of Steady States $(A, u\sqrt{A})$**.** The Jacobian matrix $J(A, u\sqrt{A})$ of the system at $(A, u\sqrt{A})$ is given as

$$J(A, u\sqrt{A}) = \begin{pmatrix} 2u^2\left(1 - \frac{A}{K}\right) & 0 \\ \dfrac{u}{2\sqrt{A}} & -1 \end{pmatrix}.$$

The matrix $J(A, u\sqrt{A})$ is a lower triangular matrix, and the eigenvalues are $\lambda_1 = 2u^2\left(1 - \frac{A}{K}\right)$ and $\lambda_1 = -1$. Thus, if $K < A$, then $\lambda_1 < 0$ and $\lambda_2 < 0$, so the point $(A, u\sqrt{A})$ is (asymptotically) stable. If $K > A$, then $\lambda_1 > 0$ and $\lambda_2 < 0$, so the point $(A, u\sqrt{A})$ is unstable. Finally, if $A = K$, then $\lambda_1 = 0$ and $\lambda_2 < 0$, and then $(A, u\sqrt{A})$ has a line of equilibria.

A.3 Stability Analysis of Steady States $(K, u\sqrt{K})$**.** The Jacobian matrix $J(K, u\sqrt{K})$ of the system at $(K, u\sqrt{K})$ is given as

$$J(K, u\sqrt{K}) = \begin{pmatrix} -u^2\left(1 - \frac{A}{K}\right) & -2u\sqrt{K}\left(1 - \frac{A}{K}\right) \\ \frac{u}{2\sqrt{K}} & -1 \end{pmatrix}.$$

The trace $tr(J)$ of this matrix is

$$tr(J) := -\left[1 + u^2\left(1 - \frac{A}{K}\right)\right].$$

Its determinant $det(J)$ is

$$det(J) := 2u^2\left(1 - \frac{A}{K}\right).$$

Also, let

$$\Delta = tr(J)^2 - 4\det(J) = \left[1 - 2u^2\left(1 - \frac{A}{K}\right)\right]^2 - 2u^2\left(1 - \frac{A}{K}\right).$$

The eigenvalues of $J(K, u\sqrt{K})$ are

$$\lambda_1 = \frac{1}{2}\left[tr(J) - \sqrt{\Delta}\right],$$
$$\lambda_2 = \frac{1}{2}\left[tr(J) + \sqrt{\Delta}\right]:$$

- Suppose $K = A$. Then $det(J) = 0$, $tr(J) = -1$, and $\Delta = 1 > 0$. It follows that $\lambda_1 = \lambda_2 = -1$. Therefore, $(K, u\sqrt{K})$ is asymptotically stable.
- Suppose $K < A$. In this case we will have $det(J) < 0$ and thus $\Delta > 0$. Since $\Delta > \left|tr(J)\right|$, we will have that $\lambda_2 > 0$. Therefore, $(K, u\sqrt{K})$ is unstable.
- Suppose $K > A$. Then $det(J) > 0$ and $tr(J) < 0$. If $\Delta > 0$, we know that the eigenvalues are real and $\lambda_1 < 0$. Moreover, we have that

$\Delta < \left|tr(J)\right| = -tr(J)$. Therefore, $\lambda_2 < 0$. Hence $(K, u\sqrt{K})$ is asymptotically stable. If $\Delta < 0$, then the eigenvalues are complex conjugates. Since their real part is $tr(J) < 0$, we conclude that $(K, u\sqrt{K})$ is asymptotically stable.

Appendix B: Stability Analysis of System 4.6

B.1 Appendix B1. The steady states are obtained when we are on the $x-$, y-, and z-isoclines. As above, on the x-isocline, we have either $y = 0$, or $f_1(x, u) - \frac{yx}{K} = 0$, or $A = \|\mathbf{W}\|^2$. On the y-isocline, we will have $y = f_2(x, y, z, u)$, and on the z-isocline, we will have $z = 1 - f_3(x, y, u)$. Now we let the Jacobian matrix at a point (x, y, z) be

$$J := J(x, y, z) = \begin{pmatrix} \alpha_1 & \alpha_2 & \alpha_3 \\ \beta_2 & \beta_2 & \beta_3 \\ \gamma_1 & \gamma_2 & \gamma_3 \end{pmatrix}.$$

where

$$\alpha_1 = \frac{\partial g_1(x, y, z)}{\partial x} = 2y\left(\frac{\partial f_1(x, u)}{\partial x} - \frac{y}{K}\right)\left(1 - \frac{A}{x}\right) + 2y\left(f_1(x, u) - \frac{yx}{K}\right)\left(\frac{A}{x^2}\right)$$

$$\alpha_2 = \frac{\partial g_1(x, y, z)}{\partial y} = \left(2f_1(x, u) - 4\frac{yx}{K}\right)\left(1 - \frac{A}{x}\right), \quad \alpha_3 = \frac{\partial g_1(x, y, z)}{\partial z} = 0,$$

$$\beta_1 = \frac{\partial g_2(x, y, z)}{\partial x} = \frac{\partial f_2(x, y, z, u)}{\partial x}, \quad \beta_2 = \frac{\partial g_2(x, y, z)}{\partial y} = -1 + \frac{\partial f_2(x, y, z, u)}{\partial y}$$

$$\beta_3 = \frac{\partial g_2(x, y, z)}{\partial z} = \frac{\partial f_2(x, y, z, u)}{\partial z}, \quad \gamma_1 = \frac{\partial g_3(x, y, z)}{\partial x} = \frac{\partial f_3(x, y, u)}{\partial x},$$

$$\gamma_2 = \frac{\partial g_3(x, y, z)}{\partial y} = \frac{\partial f_3(x, y, u)}{\partial y}, \quad \gamma_3 = \frac{\partial g_3(x, y, z)}{\partial z} = -1.$$

In the linear case, we have $f_1(x, u) = u\sqrt{x}$, $f_2(x, y, z, u) = u\sqrt{x} + zy$. With Goodall's model, we will have $f_3(x, y, u) = -uy\sqrt{x}$. It follows that

$$\alpha_1 = 2y\left(\frac{u}{2\sqrt{x}} - \frac{y}{K}\right)\left(1 - \frac{A}{x}\right) + 2y\left(u\sqrt{x} - \frac{2yx}{K}\right)\left(\frac{A}{x^2}\right),$$

$$\alpha_2 = \left(2u\sqrt{x} - 4\frac{yx}{K}\right)\left(1 - \frac{A}{x}\right), \qquad \alpha_3 = 0,$$

$$\beta_1 = \frac{u}{2\sqrt{x}}, \qquad \beta_2 = z - 1, \qquad \beta_3 = y,$$

$$\gamma_1 = \frac{uy}{2\sqrt{x}} = y\beta_1, \qquad \gamma_2 = -u\sqrt{x}, \qquad \gamma_3 = -1.$$

Now we discuss the stability of the steady states.

B.1.1 Case 1: Stability of the Line $(x, 0, 1), x > 0$. In this case, we have

$$A_0 := J(x, 0, 1) = \begin{pmatrix} 0 & 2u\sqrt{x}\left(1 - \frac{A}{x}\right) & 0 \\ \frac{u}{2\sqrt{x}} & 0 & 0 \\ 0 & -u\sqrt{x} & -1 \end{pmatrix}.$$

The eigenvalues are

$$\lambda_1 = -1, \lambda_2 = u\sqrt{1 - \frac{A}{x}}, \lambda_3 = -u\sqrt{1 - \frac{A}{x}}.$$

Since $y := v = 0 \Longrightarrow u = 0$, the eigenvalues are actually

$$\lambda_1 = -1, \lambda_2 = 0, \lambda_3 = 0.$$

Consequently, the line$(x, 0, 1)$ is always stable.

B.2 Appendix B2.

Case 2: Stability of the lines L_i, $1 \leq i \leq 2$. For L_1, we know that $y = 1$ and $z = 1 - \frac{x}{K}$, and

$$\alpha_1 = 2\left(\frac{u}{2\sqrt{x}} - \frac{1}{K}\right)\left(1 - \frac{1}{A}\right) + 2\left(u\sqrt{x} - \frac{2x}{K}\right)\left(\frac{A}{x^2}\right),$$
$$\alpha_2 = \left(2u\sqrt{x} - \frac{4x}{K}\right)\left(1 - \frac{A}{x}\right), \qquad \alpha_3 = 0,$$
$$\beta_1 = \frac{u}{2\sqrt{x}} \qquad \beta_2 = -\frac{x}{K} \qquad \beta_3 = -1,$$
$$\gamma_1 = \frac{u}{2\sqrt{x}}, \qquad \gamma_2 = -u\sqrt{x}, \qquad \gamma_3 = -1.$$

The Jacobian matrix of the system as is given at $(x, 1, 1 - \frac{x}{K})$ is given as

$$A_{21} := \begin{pmatrix} \alpha_1 & \alpha_2 & 0 \\ \beta_1 & \beta_2 & -1 \\ \beta_1 & \gamma_2 & -1 \end{pmatrix}.$$

The characteristic polynomial is $P(\lambda) = a_3\lambda^3 + a_2\lambda^2 + a_1\lambda + a_0$, where

$$a_3 = -1,$$
$$a_2 = \alpha_1 + \beta_2 - 1,$$

$$a_1 = \alpha_1(1-\beta_2) + \beta_2 - \gamma_2 + \alpha_2\beta_1,$$
$$a_0 = \alpha_1(\gamma_2 - \beta_2).$$

Case 21: $a_0 = 0$. In this case, $P(\lambda) = \lambda(-\lambda^2 + a_2\lambda + a_1)$. The roots are

$$\lambda_1 = 0, \quad \lambda_2 = \frac{1}{2}\left[a_2 - \sqrt{a_2^2 + 4a_1}\right], \quad \lambda_3 = \frac{1}{2}\left[a_2 + \sqrt{a_2^2 + 4a_1}\right].$$

Suppose that $a_2^2 + 4a_1 < 0$. If $a_2 < 0$, then λ_2 and λ_3 are complex conjugates eigenvalues with negative real parts. Thus, L_1 is a stable attractor. If $a_2 > 0$, then L_1 is unstable.

Suppose that $a_2^2 + 4a_1 > 0$. If $a_1 > 0$ and $a_2 > 0$, then λ_2 and λ_3 are real eigenvalues with $\lambda_3 > 0$. Thus, L_1 is unstable. If $a_1 < 0$ and $a_2 < 0$, then $\lambda_2 < 0$ and $\lambda_3 \leq \frac{1}{2}[a_2 + |a_2|] = 0$. It follows that L_1 is stable. If $a_1 > 0$ and $a_2 < 0$ or $a_1 < 0$ and $a_2 > 0$, then one of the eigenvalues if positive, and thus L_1 is unstable.

Case 22: $a_0 > 0$, $a_1 > 0$, $a_2 > 0$, and $a_1a_2 > a_0$. In this case, by the Routh-Hurwitz criterion (see Gradstein & Ryzhik, 2000), L_1, L_2 are stable. Since these conditions are necessary and sufficient, L_1, L_2 are unstable if they are not met.

B.2.1 Case 3: Stability of the points $\boldsymbol{B_i}$, $1 \leq i \leq 2$. **For B_1**, we know that $x = A$, $y = -1$ and $z = 1 + u\sqrt{A}$. In this case,

$$\alpha_1 = -2\left(\frac{u}{\sqrt{A}} + \frac{2}{K}\right); \quad \alpha_2 = 0, \quad \alpha_3 = 0,$$
$$\beta_1 = \frac{u}{2\sqrt{A}}, \quad \beta_2 = u\sqrt{A}; \quad \beta_3 = -1,$$
$$\gamma_1 = -\frac{u}{2\sqrt{A}}; \quad \gamma_2 = -u\sqrt{A}, \quad \gamma_3 = -1.$$

Reparameterizing as $\beta = \frac{u}{2\sqrt{A}}$ and $\gamma = u\sqrt{A}$, the Jacobian matrix of the system at $(x = A, y = -1, z = 1 + u\sqrt{A})$ is given as

$$A_{31} := \begin{pmatrix} \alpha_1 & 0 & 0 \\ \beta & \gamma & -1 \\ -\beta & -\gamma & -1 \end{pmatrix}.$$
$$\lambda_1 = \alpha_1, \quad \lambda_2 = \frac{1}{2}\left[\gamma - 1 + \sqrt{(\gamma-1)^2 + 8\gamma}\right],$$
$$\lambda_3 = \frac{1}{2}\left[\gamma - 1 - \sqrt{(\gamma-1)^2 + 8\gamma}\right].$$

Case 311: $u > 0$. In this case, $\gamma > 0$, and therefore

$$\sqrt{(\gamma-1)^2+8\gamma} = \sqrt{\gamma^2+6\gamma+1} = \sqrt{(\gamma+1)^2+4\gamma} \geq |\gamma+1| = \gamma+1.$$

It follows that $2\lambda_2 = \gamma - 1 + \sqrt{(\gamma+1)^2+4\gamma} \geq 2\gamma > 0$, and consequently, the point B_1 is unstable.

Case 312: $u < 0$. In this case, $\gamma < 0$, and therefore, $\lambda_3 < 0$. We also have

$$0 \leq \sqrt{(\gamma-1)^2+8\gamma} \leq |\gamma-1|.$$

It follows that

$$\gamma - 1 \leq 2\lambda_2 \leq \gamma - 1 + |\gamma - 1|.$$

Since $\gamma < 0 < 1$, we conclude that

$$\gamma - 1 \leq 2\lambda_2 \leq 0.$$

We finally note that $\lambda_1 = \alpha_1 \leq 0$ if $u \geq -\frac{2\sqrt{A}}{K}$. We note that

$$\max\left\{-\frac{2\sqrt{A}}{K}, -\frac{2\sqrt{A}}{2A}\right\} = -2\sqrt{A}\min\left\{\frac{1}{2A}, \frac{1}{K}\right\} = -2\sqrt{A}\max\{2A, K\}.$$

We conclude that if $-\frac{2\sqrt{A}}{K} < 2\sqrt{A}\max\{2A, K\} < u < 0$, the point B_1 is stable, and if not, it is unstable.

For B_2, we know that $x = A$, $y = 1$ and $z = 1 - u\sqrt{A}$. In this case, we have

$$\alpha_1 = 2\left(\frac{u}{\sqrt{A}} - \frac{2}{K}\right); \quad \alpha_2 = 0, \quad \alpha_3 = 0,$$
$$\beta_1 = \frac{u}{2\sqrt{A}}, \quad \beta_2 = -u\sqrt{A}; \quad \beta_3 = -1,$$
$$\gamma_1 = -\frac{u}{2\sqrt{A}}; \quad \gamma_2 = -u\sqrt{A}, \quad \gamma_3 = -1.$$

Using the same reparameterization as above, the Jacobian matrix of the system at $(x = A, y = 1, z = 1 - u\sqrt{A})$ is given as

$$A_{32} := \begin{pmatrix} \alpha_1 & 0 & 0 \\ \beta & -\gamma & -1 \\ -\beta & -\gamma & -1 \end{pmatrix}.$$

We find the eigenvalues to be

$$\lambda_1 = 0 \quad \lambda_2 = \alpha_1, \quad \lambda_3 = -\gamma - 1.$$

Case 321: $u > 0$. In this case, $\lambda_3 < 0$ since $\gamma > 0$. If $u < \frac{2\sqrt{A}}{K}$, then $\lambda_2 = \alpha_1 = 2\left(\frac{u}{\sqrt{A}} - \frac{2}{K}\right) < 0$. It follows that B_2 is stable, if not, it is unstable.

Case 322: $u < 0$. Then $\lambda_3 = -\gamma - 1 < 0$ if $\gamma > -1$, that is, if $u\sqrt{A} > -1$. Also, $\lambda_2 = \alpha_1 < 0$ if $u < 0$. In conclusion

$$\text{if } -\frac{1}{\sqrt{A}} = -\frac{2\sqrt{A}}{2A} < -2\sqrt{A}\max\{2A, K\} < u < 0, \text{ the point } B_2 \text{ is stable.}$$

References

Allee, W. C. (1949). *Principles of animal ecology*. Saunders.

Assas, L., Dennis, B., Elaydi, S., Kwessi, E., & Livadiotis, G. (2015a). A discrete-time host-parasitoid discrete model with an Allee effect. *Journal of Biological Dynamics*, *9*(1), 34–51. 10.1080/17513758.2014.982219, PubMed: 25431970

Assas, L., Dennis, B., Elaydi, S., Kwessi, E., & Livadiotis, G. (2015b). Hierarchical competition models with the Allee effect II: The case of immigration. *Journal of Biological Dynamics*, *9*(1), 288–316. 10.1080/17513758.2015.1077999, PubMed: 26394840

Assas, L., Dennis, B., Elaydi, S., Kwessi, E., & Livadiotis, G. (2016). Stochastic modified Beverton-Holt model with Allee effects II: The Cushing-Henson conjecture. *Journal of Difference Equations and Applications*, *22*(2).

Assas, L., Elaydi, S., Kwessi, E., Livadiotis, G., & Ribble, D. (2014). Competition models with Allee effects. *Journal of Difference Equations and Applications*, *20*(8), 1127–1151. 10.1080/10236198.2014.897341

Assas, L., Elaydi, S., Kwessi, E., Livadiotis, G., & Ribble, D. (2015). Hierarchical competition models with Allee effects. *Journal of Biological Dynamics*, *9*, 32–44. 10.1080/17513758.2014.923118, PubMed: 24916355

Bear, M. F., & Malenka, R. C. (1994). Synaptic plasticity: LTP and LTD. *Curr Opin Neurobiol.*, *4*, 389–399. 10.1016/0959-4388(94)90101-5, PubMed: 7919934

Bienenstock, E. L., Cooper, L. N., & Munro, P. W. (1982). Theory for the development of neuron selectivity: Orientation specificity and binocular interaction in visual cortex. *Journal of Neuroscience*, *2*, 32–48. 10.1523/JNEUROSCI.02-01-00032.1982, PubMed: 7054394

Bliss, T., & Lomo, T. (1973). Long-lasting potentiation of synaptic transmission in the dentate area of the anaesthetized rabbit following stimulation of the perforant path. *J. Physiol.*, *232*, 331–356. 10.1113/jphysiol.1973.sp010273, PubMed: 4727084

Bussey, T. (2011). Pattern separation in the hippocampus: A role for adult neurogenesis and BDNF. *Neuroscience Research*, *71*, e35. 10.1016/j.neures.2011.07.154

Cai, Y., Wang, W., & Wang, J. (2012). Dynamics of a diffusive predator-prey model—with additive Allee effect. *Inter. Jour. Biomath.*, *5*(2). 1250023.

Courchamp, F., Berec, L., & Gascoigne, J. (2008). *Allee effects in ecology and conservation*. Oxford University Press.

Dayan, P., & Abbott, L. F. (2001). *Computational and mathematical modeling of neural systems*. MIT Press.

Delitala, M., & Ferraro, M. (2020). Is the Allee effect relevant in cancer evolution and therapy? *AIMS Mathematics*, *5*, 7648–7659. 10.3934/math.2020489

Dennis, B., Assas, L., Elaydi, S., Kwessi, E., & Livadiotis, G. (2015). Allee effects and resilience in stochastic populations. *Theoretical Ecology*, *9*(3), 323–33510.1007/s12080-015-0288-2

Drapaca, C. S. (2018). Mathematical modeling of a brain-on-a-chip: A study of the neuronal nitric oxide role in cerebral microaneurysms. *Emerging Science Journal*, *6*(2).

Elaydi, S., Kwessi, E., & Livadiotis, G. (2018). Hierarchical competition models with Allee effect III: Multispecies. *Journal of Biological Dynamics*, *12*(1), 271–287. 10.1080/17513758.2018.1439537, PubMed: 29508637

Feldman, D. E. (2009). Developmental synaptic plasticity: LTP, LTD, and synapse formation and elimination. *Annu. Rev. Neurosci.*, *32*, 33–35. 10.1146/annurev.neuro.051508.135516, PubMed: 19400721

Fontanari, J. F., & Perlovsky, L. (2006). Allee effect on language evolution. In *Proceedings of the 6th International Conference of the Evolution of Language*. World Scientific.

Gradstein, I. S., & Ryzhik, I. M. (2000). *Tables of integrals, series, and products* (6th ed.). Academic Press.

Hebb, D. O. (1949). *The organization of behavior*. Wiley.

Hutchings, J. A. (2015). Thresholds for impaired species recovery. *Proceedings of the Royal Society B*, *282*, 20150654.

Johnson, K. E., Howard, G., Mo, W., Strasser, M. K., Lima, E. A. B. F., Huang, S., & Brock, A. (2019). Cancer cell population growth kinetics at low densities deviate from the exponential growth model and suggest an Allee effect. *PLoS Biology*, 17.

Konstorum, A., Hillen, T., & Lowengrub, J. (2016). Feedback regulation in a cancer stem cell model can cause an Allee effect. *Bull Mathematical Biology*, *78*, 754–785. 10.1007/s11538-016-0161-5

Kwessi, E. (2021a). A consistent estimator of nontrivial stationary solutions of dynamic neural fields. *Stats*, *4*(1), 122–137. 10.3390/stats4010010

Kwessi, E. (2021b). Discrete dynamics of dynamic neural fields. *Frontiers in Computational Neuroscience*, *15*. 10.3389/fncom.2021.699658

Liu, P. Z., & Nusslock, R. (2018a). Exercise and hippocampal neurogenesis: A dogma re-examined and lessons learned. *Neural Reg. Research*, *13*, 1354.

Liu, P. Z., & Nusslock, R. (2018b). Exercise-mediated neurogenesis in the hippocampus via BDNF. *Front. Neurosci.*, *12*.

Neufeld, Z., von Witt, W., Lakatos, D., Wang, J., Hegedus, B., & Czirok, A. (2017). The role of Allee effect in modelling post resection recurrence of glioblastoma. *PloS Computational Biology*, *13*, e1005818. 10.1371/journal.pcbi.1005818

Oja, E. (1982). Simplified neuron model as a principal component analyzer. *Journal of Mathematical Biology*, *15*, 267–273. 10.1007/BF00275687, PubMed: 7153672

Olson, A. K., Eadie, B. D., Ernst, C., & Christie, B. R. (2006). Environmental enrichment and voluntary exercise massively increase neurogenesis in the adult

hippocampus via dissociable pathways. *Hippocampus*, *16*, 250–260. 10.1002/hipo.20157, PubMed: 16411242

Perala, T., & Kuparinen, A. (2017). Detection of Allee effects in marine fishes: Analytical biases generated by data availability and model selection. *Proceedings of Royal Society B*, *284*(1861).

Sejnowski, T. J., & Tesauro, G. (1989). The Hebb rule for synaptic plasticity: Algorithms and implementations. In T. J. Sejnowski & G. Tesauro (Eds.), *Neural models of plasticity*. Academic Press.

Siegelbaum, S., & Kandel, E. R. (1991). Learning-related synaptic plasticity: LTP and LTD. *Curr Opin Neurobiol*, *1*, 113–120. 10.1016/0959-4388(91)90018-3

van Rossum, M. C. W., & Barret, A. B. (2012). Soft-bound synaptic plasticity increases storage capacity. *PloS Computational Biology*, *8*(12), e1002836. 10.1371/journal.pcbi.1002836

Xu, J., & Kang, J. (2005). The mechanisms and functions of activity-dependent long-term potentiation of intrinsic excitability. *Rev. Neurosci.*, *16*, 311–323. 10.1515/REVNEURO.2005.16.4.311, PubMed: 16519008

Received June 6, 2022; accepted December 23, 2022.